Changes in Continental Freshwater Discharge from 1948-2004

Aiguo Dai, Taotao Qian, Kevin E. Trenberth

National Center for Atmospheric Research[$],
Boulder, Colorado, USA

and John D. Milliman

School of Marine Science, College of William and Mary, Gloucester Point, VA 23062, USA

Submitted to *J. Climate*
Date: April 27, 2007

1st Revision: April 2, 2008

2nd Revision: August 21, 2008

3rd Revision: November 17, 2008

Accepted: November 18, 2008

[$] The National Center for Atmospheric Research is sponsored by the U.S. National Science Foundation.

Corresponding author address: A. Dai, National Center for Atmospheric Research, P.O. Box 3000, Boulder, CO 80307-3000, USA. Email: adai@ucar.edu

ABSTRACT

A new data set of historical monthly streamflow at the farthest downstream stations for world's 925 largest ocean-reaching rivers has been created for community use. Available new gauge records are added to a network of gauges that covers ~80 × 10^6 km^2 or ~80% of global ocean-draining land areas and accounts for about 73% of global total runoff. For most of the large rivers, the record for 1948-2004 is fairly complete. Data gaps in the records are filled through linear regression using streamflow simulated by a land surface model (CLM3) forced with observed precipitation and other atmospheric forcings that is significantly (and often strongly) correlated with the observed streamflow for most rivers. Compared with previous studies, the new data set has improved homogeneity and enables more reliable assessments of decadal and long-term changes in continental freshwater discharge into the oceans. The model-simulated runoff ratio over drainage areas with and without gauge records is used to estimate the contribution from the areas not monitored by the gauges in deriving the total discharge into the global oceans.

Results reveal large variations in yearly streamflow for most of world's large rivers and for continental discharge, but only about one-third of the top 200 rivers (including the Congo, Mississippi, Yenisey, Paraná, Ganges, Columbia, Uruguay, and Niger) show statistically significant trends during 1948-2004, with the rivers having downward trends (45) out-numbering those with upward trends (19). The interannual variations are correlated with the El Niño-Southern Oscillation (ENSO) events for discharge into the Atlantic, Pacific, Indian, and global ocean as a whole. For ocean basins other than the Arctic, and for the global ocean as a whole, the discharge data show small or downward trends, which are statistically significant for the Pacific (–10.1 km^3 yr^{-1}) and Indian Ocean (-5.4 km^3 yr^{-1}). Precipitation is a major driver for the discharge trends and large interannual to decadal variations. Comparisons with the CLM3 simulation suggest that direct human influence on annual streamflow is likely small compared with climatic forcing during 1948-2004 for

most of world's major rivers. For the Arctic drainage areas, upward trends in streamflow are not accompanied by increasing precipitation, especially over Siberia, based on available data, although recent surface warming and associated downward trends in snow cover and soil-ice content over the northern high-latitudes contribute to increased runoff in these regions. Our results are qualitatively consistent with climate model projections, but contradict an earlier report of increasing continental runoff during the recent decades based on limited records.

1. Introduction

Continental freshwater runoff or discharge is an important part of the global water cycle (Trenberth et al. 2007). Precipitation over continents partly comes from water evaporated from the oceans, and streamflow returns this water back to the seas, thereby maintaining a long-term balance of freshwater in the oceans. The discharge from rivers also brings large amounts of particulate and dissolved minerals and nutrients to the oceans (e.g., Boyer et al. 2006); thus it also plays a key role in the global biogeochemical cycles. Unlike oceanic evaporation, continental discharge occurs mainly at the mouths of world's major rivers. Therefore, it provides significant freshwater inflow locally and forces ocean circulations regionally through changes in density (Carton 1991). Continental runoff also represents a major portion of freshwater resources available to terrestrial inhabitants. As the world's population grows along with increasing demands for fresh water, interannual variability and long-term changes in continental runoff are of great concern to water managers, especially under a changing climate (Vörösmarty et al. 2000a; Oki and Kanae 2006).

There are a large number of analyses of streamflow over individual river basins (e.g., Krepper et al. 2006; Qian et al. 2006; Ye 2003; Yang et al. 2004a, 2004b; Xiong and Guo 2004), countries (e.g., Birsan et al. 2005; Groisman et al. 2001; Guetter and Georgakakos 1993; Hyvärinen 2003; Lettenmaier et al. 1994; Lindstrom and Bergstrom 2004; Lins and Slack 1999; Robson 2002; Shiklomanov et al. 2006; Zhang et al. 2001), and regions (Genta et al. 1998; Dettinger and Diaz 2000; Cluis and Laberge 2001; Lammers et al. 2001; Pasquini and Deptris 2007). Streamflow records for world's major rivers show large decadal to multi-decadal variations, but often with small secular trends (Cluis and Laberge 2001; Lammers et al. 2001; Pekárová et al. 2003; Dai et al. 2004a; Huntington 2006). However, increased streamflow during the latter half of the 20th century has been reported over regions with increased precipitation, such as many parts of the United States (Lins and Slack 1999; Groisman et al., 2001) and southeastern South America (Genta et al. 1998;

Pasquini and Deptris 2007). Decreased streamflow, in contrast, has been reported over many Canadian river basins during the last 30-50 years (Zhang et al. 2001) in response to decreased precipitation. Because large dams and reservoirs built along many of world's major rivers during the last 100 years dramatically change the seasonal flow rates (e.g., by increasing winter low flow and reducing spring/summer peak flow; Cowell and Stoudt 2002; Ye et al. 2003; Yang et al. 2004a, 2004b), trends in seasonal streamflow rates (e. g., Lammers et al., 2001) can be affected greatly by these human activities. Also, there is evidence that the rapid warming since the 1970s has caused an earlier onset of spring that induces earlier snowmelt and associated peak streamflow in the western United States (Cayan et al. 2001) and New England (Hodgkins et al. 2003) and earlier breakup of river-ice in Russian Arctic rivers (Smith 2000) and many Canadian rivers (Zhang et al. 2001).

There are, however, relatively few global analyses of river outflow to quantify variations and changes in global freshwater discharge from land into the oceans, partly because of a lack of reliable, truly global data sets (Peel and MacMahon 2006). Baumgartner and Reichel (1975) derived global maps of annual runoff and made estimates of annual continental freshwater discharge based primarily on limited streamflow data from the early 1960s analyzed by Marcinek (1964). For evaluating climate models and global analyses, new streamflow data sets have been compiled (Perry et al. 1996; Grabs et al. 1996, 2000; Bodo 2001; Dai and Trenberth 2002). As a result of these efforts, global streamflow data sets are archived at and available from several data centers, including the Global Runoff Data Centre (GRDC, http://grdc.bafg.de), the National Center for Atmospheric Research (http://dss.ucar.edu/catalogs/ranges/range550.html), and the University of New Hampshire (http://www.r-arcticnet.sr.unh.edu/v3.0/index.html). Perry et al. (1996) gave an updated estimate of long-term mean annual river discharge into the oceans by compiling published, gauge-data-based river flow estimates for 981 rivers. Fekete et al. (2002) combined streamflow data with a water balance model to derive long-term mean monthly runoff maps, from which mean

continental discharges were also estimated. Dai and Trenberth (2002) computed long-term mean monthly discharge based on downstream flow records from world's largest 921 rivers accounting for contributions from unmonitored drainage areas and the differences between the farthest downstream stations and river mouths.

There have also been attempts to quantify long-term changes in continental discharge. Probst and Tardy (1987, 1989) reported time series of freshwater discharge from each continent from the early 20th century up to 1980, based on records from only 50 major rivers (~13% of global runoff). Their results showed large decadal to multi-decadal variations and an upward trend in discharge from South America. More recently, Labat et al. (2004) analyzed records (of varying length from 4-182 years) from 221 rivers, accounting for ~51% of global runoff, but with only a small fraction of the rivers with data for the early decades (discussed further in section 4), using a wavelet transform to reconstruct monthly discharge time series from 1880-1994. Their results also show large decadal to multi-decadal variations in continental runoff and indicate a 4% increase in global runoff per 1^{o}C global surface warming. This latter result was questioned by Legates et al. (2005) and Peel and McMahon (2006) on the basis of use of insufficient streamflow data and inclusion of non-climatic changes such as human withdrawal of stream-water. Milliman et al. (2008) analyzed annual streamflow records from 137 rivers during 1951-2000 and found insignificant trends in global continental discharge.

One of the major obstacles in estimating continental discharge is incomplete gauging records or, even more daunting, unmonitored streamflow. Several methods have been applied to account for the contribution from the unmonitored areas in estimating long-term mean discharge (e.g., Perry et al. 1996; Fekete et al. 2002; Dai and Trenberth 2002), but this issue was largely ignored in long-term change analyses performed by Probst and Tardy (1987, 1989) and Labat et al.(2004). Since the monitored drainage areas vary with time, a simple summation of available streamflow records

from a selected network will likely contain discontinuities; a major issue in long-term climate data analyses (Dai et al. 2004b). Labat et al. (2004) alleviated this problem by creating a complete reconstructed time series for each river using a wavelet transform of available records.

Here we extend the climatological analysis of Dai and Trenberth (2002) to a time series analysis of continental discharge from 1948-2004. We update streamflow records for the world's major rivers with new data from several sources, and use streamflow simulated by a comprehensive land surface model (namely, the Community Land Model Ver. 3 or CLM3, see Oleson et al. 2004) forced with observed precipitation and other atmospheric forcing (Qian et al. 2006) to fill the missing data gaps through linear regression and to account for the time-varying contribution from the unmonitored drainage areas. Our goal is to create an updated monthly time series of river outflow rates from 1900-2006 for the world's largest 925 rivers for community use, to provide a reliable estimate of continental freshwater discharge from 1948-2004 that can be used as historical freshwater forcing for ocean models and in oceanic freshwater budget analyses, and to quantify variations and changes in actual (in contrast to natural) continental discharge during this time period when global warming has become pronounced and streamflow records are comparatively abundant and reliable.

We emphasize, however, that the actual streamflow and discharge examined here likely include changes induced by human activities, such as withdrawal of stream water and building dams, and thus they are not readily suitable for quantifying the effects of global warming on streamflow (as in Labat et al. 2004). Although dams and reservoirs mostly affect the annual cycle with little influence on the annual streamflow analyzed here (Ye et al. 2003; Yang et al. 2004a, 2004b; Adam and Lettenmaier 2008), combined with water withdrawal for irrigation and other uses, human activities can strongly affect river discharge (Nilsson et al. 2005; Milliman et al. 2008), which is related to sea level changes. Increased storage of water on land in reservoirs and dams may account for –0.55

mm/yr sea level equivalent (or 10,800 km^3) during the last 50 years (Chao et al., 2008), with irrigation accounting for another –0.56±0.06 mm/yr (Cazenave et al., 2000), but these are compensated for by ground water mining, urbanization, and deforestation effects. This obviously depends on the time frame, and other small contributions also exist. The net sum of land effects is now thought to be small although decadal variations may be negatively correlated with thermosteric sea level change (Ngo-Duc et al., 2005; Domingues et al., 2008).

2. Data and analysis methods

Throughout most of this work, we use the water year from October to September of the following year to improve the relationship between basin-integrated yearly precipitation and observed yearly streamflow, as snowfall (mostly in the Northern Hemisphere) of the last winter contributes to streamflow of the next spring. This also improves the correlation between observed and CLM3-simulated yearly streamflow. The actual data period for water-year discharge is from October 1948 to September 2004, in contrast to the analyzed streamflow time series, which are from January 1948 to December 2004.

a. Data sources

Dai and Trenberth (2002) merged data archived at NCAR, GRDC, and UNH and created a data set of monthly streamflow at the farthest downstream stations for world's largest 921 ocean-reaching rivers (including a few branch rivers below a downstream station on a large river). Here we updated this data set by adding available new streamflow data (mostly for recent years) from GRDC for 212 rivers, a few with different stations but scaled (using flow ratio over the common data period) to the same downstream station used in Dai and Trenberth (2002). We also added data from UNH (for Ob, Yenisey, and Lena), U.S. Geological Survey (http://nwis.waterdata.usgs.gov/nwis/) for all U.S. rivers ranked among world's top 200 rivers (see

Table 2 and Appendix of Dai and Trenberth 2002), Water Survey of Canada (http://www.wsc.ec.gc.ca/hydat/H2O/) for all top-200, Canadian rivers, an African hydrological network AOC-HYCOS (http://aochycos.ird.ne/INDEX/INDEX.HTM) for Congo and Niger (station Lokoja), and Brazilian Hydro Web (http://hidroweb.ana.gov.br/) for 17 top-200 Brazilian rivers including mid-stream stations for Paraná and Uruguay; updated to December 2006. In addition, collections of streamflow data for 121 major rivers by Milliman et al. (2008) helped improve the records for 59 rivers in this data set. The Milliman collection includes data obtained through personal contacts and it contains data for the Brahmaputra, Ganges, Mekong and other rivers that have no or very limited records in the GRDC, NCAR and UNH data archives. The updated monthly streamflow data cover the period from 1900-2006, although there are fewer records before about 1950 and after 2004. Figure 1 shows the locations of the 925 stations together with the world's major river systems as simulated by the CLM3, which has a river routing scheme.

The addition of new streamflow data from the above-mentioned sources substantially improves the record length for 154 of the world's major rivers. The average record length (after the infilling using records from nearby gauges as described below) during 1900-2006 for the world's top 10, 20, 50, 100, and 200 rivers (see Dai and Trenberth 2002) is improved to 79.9, 58.9, 54.2, and 50.0 years, respectively, in contrast to 53.8, 37.3, 38.3, and 36.4 years in Dai and Trenberth (2002). For the 57 years (1948-2004) analyzed here, the average record length (cf. Fig. 1) for the top 10, 20, 50, 100 and 200 rivers is improved to 54.2, 42.7, 39.7, and 37.6 years, respectively, in contrast to 35.3, 27.1, 27.3, and 26.9 years in Dai and Trenberth (2002). Thus, for most of the largest rivers, the data records for 1948-2004 are fairly complete (cf. section 3a). This is important, because in order to assess the long-term trends in streamflow and continental runoff the missing data in station time series should be infilled, and the estimated trends are sensitive to the infilling method when the data gaps are large.

The updated data set contains 925 ocean-reaching rivers that cover about 80×10^6 km^2 drainage areas or about 80% of the global non-ice, non-desert, non-internal-draining land areas (~100×10^6 km^2, based on the total land (133.1×10^6 km^2) and internal-drainage (17.4×10^6 km^2) areas estimated by Vörösmarty et al. 2000b and the desert area (15.9×10^6 km^2) estimated by Dai and Fung 1993) and account for about 73% of global total runoff. These numbers are considerably higher than in previous similar analyses [e.g., ~13% of global runoff in Probst and Tardy (1987, 1989), ~51% in Labat et al. (2004), and ~50% in Milliman et al. (2008)].

b. Analysis methods

Many of the station records contain data gaps although some of them are relatively short. To improve our estimates of continental discharge over the 1948-2004 period, we applied the following procedures in our analysis: 1) where possible, data gaps were filled or records were extended using data from nearby gauges through linear regression over common data periods, and the resulting records were compared with basin-integrated precipitation; 2) the remaining data gaps during 1948-2004, which were small for most of the largest rivers, were further infilled through linear regression using simulated streamflow at the station by a land model forced by observed precipitation and other forcing; 3) the streamflow data at the downstream stations were scaled up to represent river mouth flow using the ratio of simulated streamflow at the river mouth and the station; and 4) contributions of the runoff from areas not monitored by the 925 rivers were accounted for using the ratio of model-simulated runoff over the monitored and unmonitored areas. These procedures are described in detail below.

1). Use of records from nearby gauges

Streamflow records from nearby stations are often highly correlated (correlation coefficient r >0.9). To infill the data gaps and extend the records from the downstream stations used in Dai and Trenberth (2002), we applied linear regression to combine data from two stations for Amazon,

Congo, Paraná, Yukon, Uruguay, several other top-200 rivers of North and South Americas (Table 1), and some other smaller rivers from the GRDC data base. For example, Amazon streamflow data at station Obidos were available only from December1927 - July 1948 and from February 1968-present; however, we were able to download gauge height data for December 1927 – December 1974 from Taperinha (downstream of Obidos), whose monthly data are highly correlated with those of Obidos (r=0.95). This allowed us to infill the data gap from August 1948- January 1968 in the Obidos time series (Fig. 2a). This reconstructed Amazon flow time series correlates with basin-integrated precipitation better than other estimates used in the literature (Callede et al. 2002 and Milliman et al. 2008). Our tests, using gauge height data from station Manaus (as in Callede et al. 2002) yielded abnormally low flow around 1964 and resulted in lower correlation with Amazon precipitation than that using the Taperinha data. The sharp rise in the (reconstructed) Amazon flow from the mid-1960s to the early 1970s (Fig. 2a; also shown in Manaus data) is consistent with observed precipitation data (dashed line in Fig. 2a) and with an atmospheric water budget analysis using the ERA-40 reanalysis data (Betts et al. 2005), which also suggests a sharp increase in Amazonian rainfall from the mid-1960s to the early 1970s.

For Congo (Fig. 2b), streamflow data from station Kinshasa cover only 1/1903-12/1983, but we were able to extend the record to January 2001 using data from a nearby station Brazzaville (r =0.99 between flow rates at Kinshasa and Brazzaville during 1972-1983). The merged Congo time series (Fig. 2b) shows no discontinuity around 1983/1984 and is similarly correlated with basin-integrated precipitation over the entire data period. For Paraná, whose downstream flow data are unavailable to us after August 1994, we combined streamflow flow rates from two mid-stream Brazilian stations (Porto Murtinha on River Paraguai, a major tributary of Paraná, and a midstream station Guaira on Paraná) to extend the Paraná downstream record to December 2006 through regression. The combined flow record improves its correlation with Paraná's downstream flow to 0.70, which is

better than that with the CLM3-simulated flow (0.68). A mid-stream Brazilian station (Uruguaiana) on River Uruguay, whose record has a correlation of 0.96 with the Uruguay's downstream record from Dai and Trenberth (2002) (for 1/1965-12/1979 and 1991 only), was also used to extend the downstream record to cover the period from 4/1942-12/2006.

2). Infilling remaining data gaps

Despite our effort to obtain as many station records as possible, streamflow time series for many rivers still contain missing data gaps during the 1948-2004 period analyzed here, especially for many rivers in southern Asia, Africa and central America where the record length is only about 20-40 years (Fig. 1). If one simply adds up the available streamflow data for each year from individual rivers without infilling the data gaps, spurious changes in regionally averaged time series arise from the exclusion of some large rivers in the summation for certain years. A common method used in climate change analysis to handle data gaps is to assume the climatological mean or zero anomaly for the years without data (e.g., Dai et al. 1997). This is essentially a maximum likelihood method because monthly or annual anomalies for most climate variables closely follow a Gaussian distribution if the time series is stationary. When no additional information is available, this is the best assumption one can make.

As shown in Fig. 2, however, streamflow is significantly correlated with basin-integrated precipitation for many river basins. Furthermore, Qian et al. (2006) showed using a comprehensive land surface model (CLM3; Oleson et al. 2004) and observation-based atmospheric forcing (including precipitation, temperature) that it is possible to reproduce much of the variation in historical streamflow records for many of world's major rivers (cf. Fig. 5 below). Figure 3b shows that statistically significant correlations exist between the observed and CLM3-simulated streamflow for most of the world's significant rivers. For most of the world's large rivers with a flow $\geq$100 km^3 yr^{-1}, the correlation is 0.5–0.9 (Fig. 3a). One extreme exception is the Yenisey River

(the lower right point in Fig. 3a), which has an upward trend that is not captured by precipitation data and thus the CLM3 (cf. Fig. 5). However, since Yenisey has a nearly-complete record of observations from 1948-2004, this low correlation has little effect on our estimated discharge. Figure 3b shows that most of the rivers have a record length much longer than 20 years during 1948-2004. For rivers without significant correlations for the annual time series, monthly and lag correlations are explored, as described in the Appendix A.

The procedure, illustrated in Fig. 4 and described in Appendix A, makes use of the significant correlation (without the annual cycle for the majority of the rivers) between observed and CLM3-simulated streamflow (Qian et al. 2006, 2007) at the downstream stations (note that the CLM3 includes a river routing model), and through regression it fills the missing-data gaps for over 99% of the 925 rivers. We emphasize that we did not use the CLM3-simulated flow directly to fill the data gaps; instead we used a linear regression equation for each river with the simulated flow as input to estimate the flow for years without observations. Thus the mean biases and mismatch in the magnitude of variations in the CLM3-simulated flow (cf. Fig. 5) are accounted for and have little effect on the constructed flow.

To quantify the uncertainties in the regression-based infilling, the one standard deviation (s.d.) of the regression slope was used to estimate the error range in derived streamflow for each river, and this uncertainty, referred to as the regression error and which is zero for periods with observations, was integrated and included as part of the uncertainties in the estimated continental and global discharge. Another major part of the uncertainties comes from errors in streamflow measurements, which are thought to be within 10-20% (Fekete et al. 2000). However, to the extent that a large part of the measurement errors are random, they are greatly reduced in integrated discharges. To provide a quantitative estimate of this observational error, we considered the observed streamflow with the estimated streamflow derived using the regression equation and

CLM3-simulated flow as two independent samples, and used the difference between the two (multiplied by a factor of two to be conservative) as a rough estimate of the observational error. This is a very crude approximation, as the difference between the observed and estimated flow depends on how well the model simulates the flow rates at the stations, and this in turn is affected by the model physics and the forcing data. Nevertheless, this estimate of the observational error for observed streamflow, combined with the regression error (for reconstructed streamflow), provides a measure of the uncertainties for the integrated discharge.

Another source of error, which is hard to quantify and thus is not included in the error estimate, comes from poor sampling of precipitation and other atmospheric forcing during the time periods for the constructed streamflow when streamflow was not observed. This is especially true for the period after 1997 when fewer precipitation gauge records were available (Qian et al. 2006) and streamflow records for many rivers are also unavailable. Thus, our estimates of continental discharge for the period after 1997 are less reliable and should be interpreted with caution.

Despite these uncertainties, the CLM3-based infilling makes use of additional information from independent observations of precipitation, temperature, and other fields for the majority of the 925 river basins, and thus is superior to pure statistical infilling (such as used by Labat et al. 2004).

3). Adjustment to river-mouth flow

Because our focus is on continental discharge into the oceans, and the farthest downstream station for many rivers is often hundreds of kilometers away from the river mouth, we adjusted the station flow for the world's largest 200 rivers listed in Dai and Trenberth (2002) to represent river mouth outflow by multiplying the observed station flow by a ratio of the flow rates at the river mouth and the station simulated by a river routing model forced by the observation-based estimates of runoff fields from Fekete et al. (2002). More information is given in Dai and Trenberth (2002).

4). Contributions from unmonitored areas

To account for the runoff contribution from unmonitored areas (or those for which data are unavailable), which represent about 20% of the global drainage area, we used the CLM3-simulated runoff field (Qian et al. 2006, 2007) for each year to estimate the annual (for the water year Oct-Sep) discharge using the following equation (Dai and Trenberth 2002):

$$R(j) = R_o(j)\,[1 + r(j)\,A_u(j)/A_m(j)] \qquad (1)$$

where $R(j)$ is the continental discharge for 1° latitude zone j (into individual ocean basins), and $R_o(j)$ is the contribution from monitored areas (i.e. the sum of river mouth outflow of all rivers with data within latitude zone j); $A_u(j)$ and $A_m(j)$ are the unmonitored and monitored (by the stations with data) drainage areas, respectively, whose runoff enters the ocean in latitude zone j (note: $A_u(j)$ and $A_m(j)$ may contain land areas outside zone j); and $r(j)$ is the ratio of mean runoff (from the CLM3 simulation) over $A_u(j)$ and $A_m(j)$ (calculated for each 4° latitude zone); see Dai and Trenberth (2002) for details.

3. Results

a. Streamflow trends in the world's large rivers

Figure 5 shows the yearly streamflow time series from 1948-2004 from observations (thick solid line), CLM3-based infilling (thin solid line), and CLM3 simulation for world's largest 24 rivers based on adjusted river-mouth flow. Large multi-year variations are seen in most of the time series, consistent with previous analyses (Pekárová et al., 2003). For example, the Amazon River experienced high flows in the middle 1970s and low flows in the later 1960s, while the Orinoco had high flows in the early 1980s and low flows about a decade earlier. Some well-known events are evident in the streamflow time series. For example, the Sahel drought during the 1970s and 1980s is reflected by the decreasing flow in river Niger, while ENSO influence is apparent over some of the rivers, including lower flows for Amazon and higher flows for Mississippi during or following El Niño years including 1972/73, 1982/83 and 1997/98. Other atmospheric modes of variability, such

as the North Atlantic Oscillation and the Pacific Decadal Oscillation (PDO), also influence regional precipitation (Hurrell 1995; Dai et al. 1997) and thus streamflow around rims of the North Atlantic and North Pacific (Brito-Castillo et al. 2003; Milliman et al. 2008). Statistically significant long-term trends (at the 5% level, using the *t*-test described by Woodward and Gray,1993) exist during 1948-2004 only for some of the rivers shown in Fig. 5 (Table 1), namely, the Congo, Mississippi, Yenisey, Paraná, Ganges, Columbia, Uruguay, and Niger. Because of the relatively short time period, the linear trends computed are sensitive to the time period examined. For example, Milliman et al. (2008) found insignificant trends during 1951-2000 for River Columbia.

The CLM3-simulated streamflow generally follows the observed on both interannual to multi-decadal time scales (Fig. 5), resulting in significant correlations (Table 1 and Fig. 3), despite the large mean biases for some of the rivers (e.g., Uruguay, see Table 1). We emphasize that the linear regression used in infilling the data gaps removes any biases and thus they have little effect on our results here. Figure 5 also shows that the infilling (thin solid line) of the missing-data gaps using the CLM3-simulated flow through regression is more realistic than a zero-anomaly assumption. Furthermore, the CLM3 was able to capture most of the variations and long-term changes without considering direct human influences, such as dam retention and withdrawal of stream water for irrigation. This suggests that for many of world's large rivers the effects of the human activities on yearly streamflow are likely small compared with that of climate variations during 1948-2004. This is consistent with Milliman et al. (2008) who found that streamflow has decreased more than that implied by changes in precipitation only over rivers with low streamflow such as the Indus, Yellow, and Tigris-Euphrates. Since the rivers over arid regions contribute only a very small fraction to the total continental discharge, the direct effects of human activities (besides through climate change) on continental discharge is relatively small compared with climate changes. Accumulated over

many decades, however, these activities may still result in non-negligible effects on oceanic water budget (see Introduction).

The linear trends of yearly infilled streamflow for 1948-2004 for the world's largest 200 rivers are shown in Fig. 6 as a function of the long-term flow of the river, with the statistically significant (at 5% level) trends denoted by stars and insignificant ones by open circles. The majority of these rivers do not show significant trends for 1948-2004, although about one-third show significant trends of up to ±20-25% of the long-term mean per decade, and with 45 rivers with negative trends and 19 with positive trends. This is qualitatively consistent with Milliman et al. (2008) who found that out of 34 normal rivers, 24 showed no significant trends during 1951-2000, and of those with significant trends, more decreased than increased. The geographic locations of these river basins are shown in Fig. 8b.

There are also other ways to characterize long-term changes besides linear trends. For example, one can examine the difference between the mean flow averaged over an earlier and later part of the time period. Given the large climate shift around 1976/1977 associated with the shift from cold to warm PDO phase (Trenberth and Hurrell 1994; Deser et al. 2004), we examined the composite flow difference between 1948-1976 and 1977-2004. The result (not shown) revealed a smaller number (23, compared with 64 with significant linear trends) of the top-200 rivers with significant changes over the two time periods, further illustrating the sensitivity of the changes to data periods.

We emphasize that streamflow, like precipitation, has very large year-to-year variations, which make detection of changes more difficult. A linear trend is not expected for any given period but provides one measure of the change over that period. Hence a "significant" linear trend for 1948-2004 does not imply that this trend existed before or will continue after this period.

b. Changes in continental discharge

Following Dai and Trenberth (2002), we integrated the discharge for each 4^o lat. × 5^o lon. coastal box for each individual water year, and then computed the linear trend at each coastal box. Although Fig. 5 suggests that the effect of human activities is likely secondary compared with climate effects for most of world's large rivers, we did not attempt to exclude any human-induced changes because our focus is on the actual flow into the oceans. Because human interference is likely to decrease flows, increases are more attributable to climatic forcings.

Figure 7 shows the time series of the yearly (Oct-Sep) fresh water discharge into the ocean basins estimated using the observed streamflow from the 925 rivers with missing-data gaps infilled using CLM3-simulated flow through regression (solid line) and infilled using the long-term mean (dashed line). Figure 7 is designed to show the differences between the two different estimates and does not include the contribution from the unmonitored areas. Noticeable differences exist between the estimates using the two infilling methods, especially for the Indian Ocean, although they are small because the updated streamflow records are fairly complete for the majority of the large rivers. Thus, the conclusions regarding discharge trends in this study are insensitive to the infilling methods, but this does not apply to other studies that have more missing data.

Figure 8 shows the water-year discharge trend around the coasts during 1948-2004 (panel a) and its implied runoff trend over the corresponding drainage areas (panel b, i.e., by dividing the downstream flow trend with the upstream drainage area), together with their confidence levels based on the *t*-test (panels g-h). Here the gridded coastal discharge trend, which may differ from the streamflow trend for individual rivers shown in Fig. 5, was distributed evenly over its drainage area using the digital river network of Vörösmarty et al. (2000b). Statistically significant positive trends occur over the coasts around the Arctic Ocean, especially over eastern Russia and Canada. Another positive trend is around the Gulf of Mexico mainly from the Mississippi River basin. Decreasing trends over the central Africa (mainly Congo), West Africa (the Sahel), and southeastern Australia

are statistically significant. On the other hand, the trends over most South American coasts are insignificant. The magnitude and statistical significance of the trends are sensitive to the exact time period examined and, in particular, whether the data for the most recent years are included. For example, the upward trends for both the Mississippi and Paraná leveled off after 1997, perhaps in response to a subtle shift in the PDO, and thus analyses with data only up to the late 1990s (e.g., Milliman et al. 2008) reveal larger trends than shown here.

To help examine the causes behind the discharge and runoff trends, Fig. 8c-f show the trends during the same period in observed surface air temperature and precipitation (both from Qian et al. 2006), and CLM3-simulated snow-cover and soil-ice water content. Widespread decreases in precipitation over Africa, southeastern Asia, and eastern Australia coincide with decreased runoff in these regions, while increases in precipitation over much of the U.S., Argentina, and northwestern Australia are consistent with runoff increases in these areas. However, the runoff increases over central and eastern Russia can not be explained by the decreased precipitation (Fig. 8b, d), as noted previously (Berezovskaya et al. 2004; Milliman et al. 2008). Other precipitation data sets such as those from the Climate Research Unit (CRU, http://www.cru.uea.ac.uk/cru/data/) and the Global Precipitation Climatology Centre (http://www.dwd.de/en/FundE/Klima/KLIS/int/GPCC/GPCC.htm) show similar trends over these regions. We notice that rain-gauge data are sparse in all the precipitation products over many regions such as the Siberia, tropical Africa, and Amazon, and thus they may contain large sampling errors. The CLM3 simulation suggests that large surface warming over the Siberia (Fig. 8c) has caused melting and thus decreases in surface snow cover (Fig. 8e) and soil ice (Fig. 8f), which can contribute to increases in runoff. The potential contribution of thawing of the permafrost, as well as other factors (e.g., changes in evaporation), to the observed increases in runoff into the Arctic Ocean has been discussed by Adam and Lettenmaier (2008).

Figure 9 shows the integrated freshwater discharge (solid line, including contributions from unmonitored areas) into the individual and global oceans, together with an estimate of the uncertainties (shading, cf. Section 3). Large interannual and decadal variations are evident in the discharge into all the oceans. Some of these variations are correlated with the ENSO, as represented by the Niño3.4 SST index, which is the normalized sea surface temperature anomalies averaged over 160°E-90°W and 5°S-5°N (dashed line in Fig. 9; updated from Trenberth 1997) averaged over a 12-month period that leads the discharge average period by four months for the Atlantic Ocean (Fig. 9a), and lags the discharge by one month for the Pacific Ocean (Fig. 9b), by five months for the Indian Ocean (Fig. 9c), and by one month for the global ocean as a whole (Fig. 9f). These differences in the time lag result from the time lag between the index and ENSO-induced precipitation anomalies which varies spatially (Trenberth et al. 2002). The correlation with the Niño3.4 SST index is strongest for the Pacific basin (correlation coefficient r = -0.61, $p < 0.01$), as ENSO greatly affects precipitation over land around the Pacific rim (Dai and Wigley 2000). El Niños tend to reduce streamflow for some Atlantic-draining rivers such as the Amazon, Orinoco, and Niger, but increase the flow in rivers such as the Mississippi, Paraná, and Uruguay (cf. Fig. 5), resulting in relatively weak correlation (r = -0.50, p< 0.01, at the above given lag) between the Atlantic discharge and the ENSO index (Fig. 9a). Even for the global discharge, the correlation with ENSO is fairly strong (r = -0.66, $p < 0.01$). No significant correlation is found between ENSO indices and the discharge into the Arctic and the Mediterranean and Black Seas (Fig. 5d-e), which is not surprising given that ENSO's influence on precipitation is mostly at low- and mid-latitudes (Dai and Wigley 2000).

In addition to the large variations, Fig. 9 also shows an upward trend in the discharge into the Arctic Ocean (slope b = 8.2 km^3 yr^{-1} or 0.26 × 10^{-3} Sv yr^{-1}, $p < 0.01$; 1 Sv = 10^6 m^3 s^{-1}), and downward trends for the Pacific (b = –9.4 km^3 yr^{-1} or –0.30 × 10^{-3} Sv yr^{-1}, p =0.01). Trends in the

discharge into the other basins are negative but statistically insignificant, including the global oceans as a whole (b = –6.96 km^3 yr^{-1} or –0.23 × 10^{-3} Sv yr^{-1}, p = 0.40). While the increasing trend in the Arctic discharge is in agreement with previous reports (Peterson et al. 2002), the negative trends for the other ocean basins are in sharp contrast to the perceived but unjustified notion that global continental discharge should increase as the climate becomes warmer and the global hydrological cycle intensifies (Milly et al. 2002; Labat et al. 2004; Huntington 2006). On the other hand, the decreasing runoff and discharge trends are consistent with the trends in the Palmer Drought Severity Index of the last 50 years or so (Dai et al. 2004a), which suggests a general drying over global land.

Precipitation decreases over many of the low- and mid-latitude land areas are the causes for the decline in runoff during 1948-2004 (Fig. 8). To further illustrate the relationship with precipitation changes, Figure 10 compares the drainage-area integrated precipitation (dashed line) with the discharge time series (solid line, same as in Fig. 9). As expected, the discharge time series are significantly correlated with precipitation, especially for the Pacific (r = 0.62, p < 0.01) on both interannual and longer time scales, except for the Indian and Arctic Ocean, where precipitation does not show an upward trend until the late 1990s (Fig. 10d). The weak correlation for the Indian Ocean reflects the poor sampling for both streamflow and precipitation in southern Asia and eastern Africa.

Since the ratio of runoff to precipitation (i.e. the runoff coefficient) varies from near zero over deserts to close to one over wet areas, one may expect that multiplying precipitation by the long-term runoff coefficient (based on the runoff maps from Fekete et al. 2002 and precipitation from Qian et al. 2006) before the area-integration might improve the correlation between precipitation and the discharge. We found that this is true only for the relatively dry Mediterranean and Black Sea drainage basin (r increased from 0.38 to 0.61). For the other basins and global land as a whole,

the correlation did not change much, suggesting that the runoff coefficient variations themselves are important.

Extremely high continental discharge occurred in 1974 (Figs. 9-10), a La Niña year, and record low discharge happened in 1992, an El Niño year, for the global and some of the individual oceans (mainly the Atlantic). Figure 11 shows the maps of the observed precipitation and CLM3-simulated runoff anomalies (relative to 1948-2004 mean) for the water years 1974 and 1992. Large positive precipitation anomalies occurred in 1974 over Australia, southern and central Africa, tropical South America, much of the central and eastern United States and Canada, and north to the Bay of Bengal. Overall, 1974 was a wet year over most of the continents, as indicated by the predominant cold colors in Fig. 11a and 11c. On the other hand, 1992 was an exceptionally dry year for most of the land areas, especially over the low latitudes such as the Indonesia-Australia region, southern Asia, western and southern Africa, tropical South America, much of Europe, western Canada and the Northwest U.S. A regression of the runoff and precipitation with ENSO indices (Trenberth and Dai 2007) confirms that a large part of these precipitation anomalies is induced by the cold ENSO event in 1974 and the warm event in 1992. However, the precipitation and thus the discharge and runoff anomalies are also influenced by other factors, in particular the huge volcanic eruption of Mt. Pinatubo in June 1991 (Trenberth and Dai 2007), as the post 1991 anomalies are more widespread and larger in magnitude than those associated with typical ENSO events or even the strongest El Niños in 1982 and 1997.

4. Summary and concluding remarks

We have updated the global monthly streamflow data set of Dai and Trenberth (2002) with additional new records for a number of world's major rivers. The average record length for 1948-2004 for the world's top 10, 20, 50, 100 and 200 rivers has been improved to 54.2, 42.7, 39.7, and

37.6 years, respectively, after infilling data gaps using nearby station data. The remaining data gaps were infilled with estimates derived using the CLM3-simulated streamflow through regression, which makes use of precipitation data and the correlation between precipitation and streamflow. This has resulted in a new global data set of continuous monthly streamflow from 1948-2004 at the farthest downstream stations for world's 925 largest ocean-reaching rivers. This network of gauges covers ~80 × 10^6 km^2 or ~80% of global ocean-draining areas and accounts for about 73% of global total runoff, although some data gaps (before the infilling) exist for many of the gauge records which reduce the coverage for some individual years.

The CLM3-simulated runoff ratio [cf. eq. (1)] was used to estimate the contribution from the drainage areas not monitored by the 925 rivers, whereas the ratio of the simulated flow at the river mouth and the farthest downstream station by a river routing model forced with observation-based long-term runoff fields (from Fekete et al. 2002) was used to adjust the station flow to represent river mouth outflow. Therefore, our estimates of the continental discharge include runoff from all land areas except Antarctica (~2,613 km^3 yr^{-1} according to Jacobs et al. 1992) and Greenland. There is also a small coastal discharge through groundwater (estimated as 2,200 km^3 yr^{-1} globally by Korzun et al 1977), although part of this groundwater discharge is included in our estimates of the discharge contribution from the unmonitored areas because the groundwater has to come from surface (runoff) water on a long-term basis. For comparison, our estimate of long-term global discharge is about 37,288 km^3 yr^{-1} or 1.18 Sv (see Table 4 of Dai and Trenberth 2002, excluding Antarctica and Greenland).

Although our data set contains records before 1948 and up to 2006 for many rivers, our analysis here focused on the 1948-2004 period when the record is most complete for the majority of the rivers. Comparisons with the CLM3-simulated streamflow, which does not include any direct human influence (other than through human-induced climate changes), suggest that for most of

world's large rivers the effect of the human activities on *yearly* streamflow (including its trend) are likely small compared with that of climate changes since 1948 (but human activities do have other impacts, see Introduction). Consistent with previous analyses, large interannual to decadal variations are seen in the streamflow in most of world's major rivers. However, statistically significant trends up to ±20-25% per decade during 1948-2004 exist only for about one third of world's top 200 rivers, including the Congo, Mississippi, Yenisey, Paraná, Ganges, Columbia, Uruguay, and Niger, with the rivers having downward trends (45) out-numbering those with upward trends (19). The magnitude and statistical significance of the trends are sensitive to the time period examined.

Large interannual to decadal variations in continental discharge are correlated with ENSO events for the discharge into the Atlantic, Pacific, Indian, and global oceans as a whole, but not with discharges into the Arctic Ocean and the Mediterranean and Black Seas, suggesting that ENSO-induced precipitation anomalies over the low- and mid-latitude land areas are a major cause for the variations in continental discharge, consistent with many regional analyses (e.g., Kahya and Dracup, 1993; Pasquini and Depetris 2007) and precipitation analyses (Dai and Wigley 2000; Gu et al. 2007).

Consistent with previous reports, we found a large upward trend in the yearly discharge into the Arctic Ocean (8.2 $km^3\ yr^{-1}$) from 1948-2004. For the other ocean basins and the global oceans as a whole, the discharge has downward trends, which are statistically significant for the Pacific (–9.4 $km^3\ yr^{-1}$). Aside from the Arctic and Indian Ocean, where precipitation data contain large uncertainties, precipitation is significantly correlated with discharge, suggesting that precipitation change is a major cause for the discharge trends and large interannual to decadal variations. Seasonal trends are not examined here as they are more susceptible to non-climatic effects such as dams, reservoirs and irrigation, which makes their interpretation more difficult.

Our results are consistent with the wide spread drying during recent decades over global land found by Dai et al. (2004a). They are also consistent with the insignificant trend in global discharge during 1951-2000 found by Milliman et al. (2008). However, our results contradict the notion that global runoff has increased during the recent decades (Labat et al. 2004) and that enhanced water use efficiency by plants has contributed to the runoff increase (Gedney et al. 2006) (see Appendix B for more details on these two studies). Multi-model ensemble predictions by current climate models show consistent increases in streamflow only for the northern high-latitude rivers (Nohara et al. 2006), because projected precipitation changes are far from uniform increases; there are widespread decreases in the subtropics (e.g., Dai et al. 2001; Sun et al. 2007; IPCC 2007). The downward trends in low- and mid-latitude streamflow records are consistent with the general drying trend over global land during the last 50 years or so (Dai et al. 2004a).

The reduced runoff in low- and mid-latitudes has increased the pressure on limited freshwater resources over the world, especially as the demand increases with world's population growth (Vörösmarty et al. 2000a). This problem is likely to continue or even worsen in the coming decades based on the multi-model predictions of precipitation and streamflow of the 21st century (IPCC 2007).

Acknowledgments: This study was partly supported by NSF Grant #ATM-0233568 and NCAR's Water Cycle Program. The streamflow data set will be freely available from http://www.cgd.ucar.edu/cas/catalog/ after the publication of this paper.

Appendix A: Estimating discharge when observations are missing

Here we make use of the significant correlation between observed and CLM3-simulated streamflow (cf. Figs. 3 and 5) for the majority of the 925 rivers to estimate the river outflow rates

for periods without data. The procedure for this reconstruction is illustrated in Fig. 4. We first divided the streamflow records into two groups: Group A (top half in Fig. 4) with a total record length not shorter than 180 months (or 15 years, may contain gaps) and Group B (lower half in Fig. 4) with less than 180 months of records. This 15–year limit was chosen based on the consideration of the minimum length of records required for a reliable regression and the overall record length in the data set. For Group A, we computed the correlation coefficient (R) between the observed and simulated twelve monthly and one annual streamflow time series separately at the farthest downstream station for each river. If R was statistically significant at the 5% level, then a linear regression between the observed and simulated streamflow time series (for each month and the annual mean) was used to derive streamflow rates for the months without data using the simulated flow as input (annual values were estimated using the annual regression). When the correlation for some monthly time series was insignificant but there were 8 or more other months with significant correlation and valid regression, then data gaps in those monthly time series without regression were filled using spline interpolation of observed or estimated streamflow of the other months. As shown in Fig. 4, there were about 419 (or 45%) rivers whose annual and monthly streamflow time series were significantly correlated with the CLM3-simulated flow for at least 8 or more of the 12 months. For the remaining rivers in Group A (i.e., those did not fit into categories c00 and c01 in Fig. 4), a correlation (R_{am}) using the 12-month-combined time series of streamflow from the observations and the CLM3 simulation was computed. If R_{am} was significant at the 5% level, then a regression between the all-month time series was used to fill the missing monthly gaps. Annual values were derived from annual regression in this case, i.e., c02 in Fig. 4. If R_{am} was insignificant at zero lag, but it became significant and maximized when we introduced a time lag from -5 to +5 months, then a regression was done at that lag and used to fill the monthly data gaps (c03).

Categories c02 and c03 were repeated for those rivers in Group A whose annual time series were not significantly correlated (c05 and c06).

There were about 27.6% of the rivers falling into Group B, with a record shorter than 180 months. For this group, the correlation and regression were done for 12-month-combined time series only (with the annual cycle included). If the simultaneous correlation was significant, then a regression was used to fill the monthly gaps (c08, 25.8%); otherwise, the maximum lag correlation (within ± 5 months) was sought and a regression was used to fill the monthly data gaps if the maximum lag correlation was significant (c09, 1.2%). Annual values were derived from the monthly data or estimates for rivers in Group B. We realize that the inclusion of the annual cycle in for Group B rivers may enhance the correlation; however, we do not think it has significant effects on the discharge estimates because these are mostly small rivers.

Appendix B: Reasons for different findings by previous studies

Here we explore why Labat et al. (2004) reached different conclusions. Labat et al. (2004) obtained monthly streamflow data for 221 rivers from the GRDC and another source (for Amazon only) which account for about half of the global discharge for years when all the rivers have observations. However, they used only ten so-called reference rivers for reconstruction of the complete time series from 1880-1925 and considered the variations only at monthly, annual, and multi-year time scales during the reconstruction through a wavelet transform, so that decadal and longer variations were excluded. Global discharge time series were derived by summing up these ten time series, and a constant, scaling coefficient was used to account for the complete continental surface. This scaling coefficient was derived from the outdated long-term mean global and continental discharge estimates by Baumgartner and Reichel (1975) (see Dai and Trenberth 2002 for problems in the Baumgartner and Reichel estimates). Finally, the estimate was scaled up by a factor of 1/0.89 to

account for the contribution from Australia and Antarctica. In essence, the variations and trends in the global discharge time series of Labat et al. (2004) were derived completely from streamflow records of only ten rivers with constant scaling for 1880-1925 period, and their conclusion was based on the trend estimated for the entire 1880-1994 period. Our experience with the available streamflow records suggest that it is very difficult, if not impossible, to derive reliable estimates of global continental discharge for decades before the 1940s simply because most of the world's major rivers do not have observations during the first half of the 20th century (let alone the 19th century). Hence, our estimate of discharge trends for 1948-2004 is not comparable with Labat et al. (2004)'s estimate for ~1875-1994.

Gedney et al. (2006) first accepted the discharge increase reported by Labat et al. (2004) as the truth and applied a land surface model, similar to the CLM3, forced with Climate Research Unit monthly surface data which included climatological values for many land areas, and climatological winds to attribute the discharge increases to several factors. They concluded that enhanced water use efficiency by plants is a big contributor to the runoff increase. Neither our CLM3 simulation, which is very similar to the model simulations done by Gedney et al. (2006) except we used a different forcing data set, nor our analysis of the streamflow records, show significant upward trends in global discharge during the last five decades when atmospheric CO_2 has been steadily increasing. This suggests that the conclusion of Gedney et al. (2006) is model and data-dependent.

References

Adam, J. C. and D. P. Lettenmaier, 2008: Application of new precipitation and reconstructed streamflow products to streamflow trend attribution in northern Eurasia. *J. Climate*, **21,** 1807-1828.

Baumgartner, A., and E. Reichel, 1975: *The World Water Balance*. Elsevier, 179 pp.

Berezovskaya, S., D. Q. Yang, and D. L. Kane, 2004: Compatibility analysis of precipitation and runoff trends over the large Siberian watersheds. *Geophys. Res. Lett.*, **31,** L21502, doi: 10.1029/2004GL021277.

Betts, A. K., J. H. Ball, P. Viterbo, A. G. Dai, and J. Marengo, 2005: Hydrometeorology of the Amazon in ERA-40. *J. Hydrometeorol.*, **6,** 764-774.

Birsan, M. V., P. Molnar, P. Burlando, and M. Pfaundler, 2005: Streamflow trends in Switzerland. *J. Hydrology*, **314,** 312-329.

Bodo, B. A., 2001: Annotations for monthly discharge data for world rivers (excluding former Soviet Union), 85 pp. [Available on-line from http://dss.ucar.edu/datasets/ds552.1/docs/]

Boyer, E. W., R. W. Howarth, J. N. Galloway, F. J. Dentener, P. A. Green, and C. J. Vörösmarty, 2006: Riverine nitrogen export from the continents to the coasts. *Glob. Biogeochem. Cycles*, **20,** GB1S91, doi:10.1029/2005GB002537.

Brito-Castillo, L., A. V. Douglas, A. Leyva-Contreras, and D. Lluch-Belda, 2003: The effect of large-scale circulation on precipitation and streamflow in the Gulf of California continental watershed. *Intl. J. Climatol.*, **23,** 751-768.

Callede, J., J. L. Guyot, J. Ronchail, M. Molinier, and E. De Oliveira, 2002: The River Amazon at Obidos (Brazil): Statistical studies of the discharges and water balance. *Hydrol. Sci. J.*, **47,** 321-333.

Carton, J. A., 1991: Effect of seasonal surface fresh-water flux on sea-surface temperature in the tropical Atlantic Ocean. *J. Geophys. Res.*, **96,** 12593-12598.

Cayan, D. R., S. A. Kammerdiener, M. D. Dettinger, J. M. Caprio, and D. H. Peterson, 2001: Changes in the onset of spring in the western United States. *Bull. Amer. Meteor Soc.*, **82,** 399-415.

Cazenave, A., F. Remy, K. Dominh, and H. Douville, 2000: Global ocean mass variation, continental hydrology and the mass balance of Antarctica ice sheet at seasonal time scale. *Geophys. Res. Lett.*, **27,** 3755-3758.

Chao, B. F., Y. H. Wu, and Y. S. Li, 2008: Impact of artificial reservoir water impoundment on global sea level. *Science*, **320,** 212-214.

Cluis, D., and C. Laberge, 2001: Climate change and trend detection in selected rivers within the Asia-Pacific region. *Water International*, **26,** 411-424.

Cowell, C. M., and R. T. Stoudt, 2002: Dam-induced modifications to upper Allegheny River streamflow patterns and their biodiversity implications. *J. Amer. Water Res. Assoc.*, **38,** 187-196.

Crow, E. L., F. A. Davis, and M. W. Maxfield, 1960: *Statistical Manual*. Dover Publications, Inc., New York, 288 pp.

Dai, A., and I. Fung, 1993: Can climate variability contribute to the "missing" CO2 sink? *Global Biogeochem. Cycles*, **7**,599-609.

Dai, A., I. Y. Fung, and A. D. Del Genio, 1997: Surface observed global land precipitation variations during 1900-88. *J. Climate*, **10,** 2943-2962.

Dai, A., and K. E. Trenberth, 2002: Estimates of freshwater discharge from continents: Latitudinal and seasonal variations. *J. Hydrometeorol.*, 3, 660-687.

Dai, A., K. E. Trenberth, and T. T. Qian, 2004a: A global dataset of Palmer Drought Severity Index for 1870-2002: Relationship with soil moisture and effects of surface warming. *J. Hydrometeor.*, **5,** 1117-1130.

Dai, A., P. J. Lamb, K. E. Trenberth, M. Hulme, P. D. Jones, and P. Xie, 2004b: The recent Sahel drought is real. *Intl J. Climatol.,* **24**, 1323-13331.

Dai, A., and T. M. L. Wigley, 2000: Global patterns of ENSO-induced precipitation. *Geophys. Res. Lett.*, **27**, 1283-1286.

Dai, A., T.M.L. Wigley, B.A. Boville, J.T. Kiehl, and L.E. Buja, 2001: Climates of the 20th and 21st centuries simulated by the NCAR Climate System Model. *J. Climate,* **14**, 485-519.

Deser, C., A. S. Phillips, and J. W. Hurrell, 2004: Pacific interdecadal climate variability: Linkages between the tropics and the North Pacific during boreal winter since 1900. *J. Climate*, **17,** 3109-3124.

Dettinger, M. D., and H. F. Diaz, 2000: Global characteristics of stream flow seasonality and variability. *J. Hydrometeor.*, **1,** 289-310.

Domingues, C. M., J. A. Church, N. J. White, P. J. Gleckler, S. E. Wijffels, P. M. Barker, and J. R. Dunn, 2008: Improved estimates of upper-ocean warming and multi-decadal sea-level rise. *Nature*, **453,** 1090-1093.

Fekete, B. M., C. J. Vörösmarty, and W. Grabs, 2000: Global composite runoff fields based on observed river discharge and simulated water balances. Global Runoff Data Centre Rep. No.22, Koblenz, Germany, 39 pp. [Available online at http://www.bafg.de/grdc.htm]

Fekete, B. M., C. J. Vörösmarty, and W. Grabs, 2002: High-resolution fields of global runoff combining observed river discharge and simulated water balances. *Global Biogeochem. Cycles*, **16,** doi:10.1029/1999GB001254.

Gedney, N., P. M. Cox, R. A. Betts, O. Boucher, C. Huntingford, and P. A. Stott, 2006: Detection of a direct carbon dioxide effect in continental river runoff records. *Nature*, **439,** 835-838.

Genta, J. L., G. Perez-Iribarren, and C. R. Mechoso, 1998: A recent increasing trend in the streamflow of rivers in southeastern South America. *J. Climate*, **11,** 2858-2862.

Grabs, W.E., T. de Couet, and J. Pauler, 1996: Freshwater fluxes from continents into the world oceans based on data of the global runoff data base. Global Runoff Data Centre (GRDC) Rep. No. 10, Germany, 49 pp. + annex 179 pp. [Available from GRDC, Fed. Inst. of Hydrology, Kaiserin-Augusta-Anlagen 15-17, D-56068 Koblenz, Germany]

Grabs, W.E., F. Portmann, and T. de Couet, 2000: Discharge observation networks in Arctic regions: Computation of the river runoff into the Arctic Ocean, its seasonality and variability. In: *The Freshwater Budget of the Arctic Ocean*, Lewis, E.L. et al. (eds.), Kluwer Academic Publ., Dordrecht, pp. 249-267.

Groisman, P. Y., R. W. Knight, and T. R. Karl, 2001: Heavy precipitation and high streamflow in the contiguous United States: Trends in the twentieth century. *Bull. Amer. Meteor. Soc.*, **82,** 219-246.

Gu, G., R. F. Adler, G. J. Huffman and S. Curtis, 2007: Tropical rainfall variability on interannual-to-interdecadal/longer-time scales derived from the GPCP monthly product. *J. Climate,* **20**, 4033-4066.

Guetter, A. K., and K. P. Georgakakos, 1993: River Outflow of the Conterminous United-States, 1939-1988. *Bull. Amer. Meteor. Soc.*, **74,** 1873-1891.

Hodgkins, G. A., R. W. Dudley, and T. G. Huntington, 2003: Changes in the timing of high river flows in New England over the 20th Century. *J. Hydrology*, **278,** 244-252.

Huntington, T. G., 2006: Evidence for intensification of the global water cycle: Review and synthesis. *J. Hydrology*, **319,** 83-95.

Hurrell, J. W., 1995: Decadal Trends in the North-Atlantic Oscillation - Regional Temperatures and Precipitation. *Science*, **269,** 676-679.

Hyvärinen, V., 2003: Trends and characteristics of hydrological time series in Finland. *Nordic Hydrology*, **34,** 71-90.

Kahya, E., and J. A. Dracup, 1993: United-States Streamflow Patterns in Relation to the El-Nino Southern Oscillation. *Water Resources Res.*, **29,** 2491-2503.

Korzun, V. I., A. A. Sokolov, M. I. Budyko, K. P. Voskrensensky, G. P. Kalinin, A. A. Konoplyantsev, E. S. Korotkevich, and M. I. Lvovich, 1977: Atlas of the world water balance. UNESCO, Paris, 36 pp. + 65 maps.

Krepper, C. M., N. O. Garcia, and P. D. Jones, 2006: Paraguay river basin response to seasonal rainfall. *Intl J. Climatol.*, **26,** 1267-1278.

IPCC 2007: Climate Change 2007: *The Physical Science Basis*. Contribution of WG 1 to the Fourth Assessment Report of the Intergovernmental Panel on Climate Change. [S. Solomon, et al. (eds)]. Cambridge University Press. Cambridge, U. K., and New York, NY, USA, 996pp.

Jacobs, S. S., H. H. Helmer, C. S. M. Doake, A. Jenkins, and R. M. Frolich, 1992: Melting of ice shelves and the mass balance of Antarctica. *J. Glaciology*, **38,** 375-387.

Labat, D., Y. Goddéris, J. L. Probst, and J. L. Guyot, 2004: Evidence for global runoff increase related to climate warming. *Adv. Water Res.*, **27,** 631-642.

Lammers, R. B., A. I. Shiklomanov, C. J. Vörösmarty, B. M. Fekete, and B. J. Peterson, 2001: Assessment of contemporary Arctic river runoff based on observational discharge records. *J. Geophys. Res.*, **106,** 3321-3334.

Legates, D. R., H. F. Lins, and G. J. McCabe, 2005: Comments on "Evidence for global runoff increase related to climate warming" by Labat et al. *Adv. Water Res.*, **28,** 1310-1315.

Lettenmaier, D. P., E. F. Wood, and J. R. Wallis, 1994: Hydro-climatological trends in the continental United States, 1948-88. *J. Climate*, **7,** 586-607.

Lindstrom, G., and S. Bergstrom, 2004: Runoff trends in Sweden 1807-2002. *Hydrologic Science J.*, **49,** 69-83.

Lins, H. F., and J. R. Slack, 1999: Streamflow trends in the United States. *Geophys. Res. Lett.*, **26,** 227-230.

Marcinek, J., 1964: The River Discharge from Land Surface over the Globe and its Distribution in 5^{o} Zones (in German). *Bull. Inst. Water Management*, **21,** 204 pp.

Milliman, J. D., K.L. Farnsworth, P.D. Jones, K.H. Xu, and L.C. Smith, 2008: Climatic and anthropogenic factors affecting river discharge to the global ocean, 1951-2000. *Global Planetary Change*, in press.

Milly, P. C. D., R. T. Wetherald, K. A. Dunne, and T. L. Delworth, 2002: Increasing risk of great floods in a changing climate. *Nature*, **415,** 514-517.

Mitchell, T. D. and P. D. Jones, 2005: An improved method of constructing a database of monthly climate observations and associated high-resolution grids. *Intl. J. Climatol.*, **25,** 693-712.

Ngo-Duc, T., K. Laval, J. Polcher, A. Lombard, and A. Cazenave, 2005: Effects of land water storage on global mean sea level over the past half century. *Geophys. Res. Lett.*, **32,** L09704, doi:10.1029/2005GL022719.

Nilsson, C., C. A. Reidy, M. Dynesius, and C. Revenga, 2005: Fragmentation and flow regulation of the world's large river systems. *Science*, **308,** 405-408.

Nohara, D., A. Kitoh, M. Hosaka, and T. Oki, 2006: Impact of climate change on river discharge projected by multimodel ensemble. *J. Hydrometeor.*, **7,** 1076-1089. Oleson, K. W., Y. Dai, G. Bonan, M. Bosilovich, R. Dickinson, P. Dirmeyer, F. Hoffman, P. Houser, S. Levis, G.-Y. Niu, P. Thornton, M. Vertenstein, Z.-L. Yang, and X. Zeng, 2004: Technical Description of the Community Land Model (CLM). *NCAR/TN-461+STR***,** 186 pp.

Oki, T. and S. Kanae, 2006: Global hydrological cycles and world water resources. *Science*, **313,** 1068-1072.

Pasquini, A. I., and P. J. Depetris, 2007: Discharge trends and flow dynamics of South American rivers draining the southern Atlantic seaboard: An overview. *J. Hydrol.*, **333,** 385-399.

Peel, M. C. and T. A. McMahon, 2006: Continental runoff - A quality-controlled global runoff data set. *Nature*, **444,** E14-E14.

Pekárová, P., P. Miklánek, and J. Pekár, 2003: Spatial and temporal runoff oscillation analysis of the main rivers of the world during the 19th–20th centuries. *J. Hydrology*, **274,** 62-79.

Perry, G. D., P. B. Duffy, and N. L. Miller, 1996: An extended data set of river discharges for validation of general circulation models. *J. Geophys. Res.*, **101,** 21339-21349.

Peterson, B. J., R. M. Holmes, J. W. McClelland, C. J. Vörösmarty, R. B. Lammers, A. I. Shiklomanov, I. A. Shiklomanov, and S. Rahmstorf, 2002: Increasing river discharge to the Arctic Ocean. *Science*, **298,** 2171-2173.

Probst, J. L. and Y. Tardy, 1987: Long-range streamflow and World continental runoff fluctuations since the beginning of this century. *J. Hydrology*, **94,** 289-311.

Probst, J. L. and Y. Tardy, 1989: Global runoff fluctuations during the last 80 Years in relation to world temperature-change. *American J. Sci.*, **289,** 267-285.

Qian, T., A. Dai, K. E. Trenberth, and K. W. Oleson, 2006: Simulation of global land surface conditions from 1948-2004. Part I: Forcing data and evaluation. *J. Hydrometeor.,* **7**, 953-975.

Qian, T., A. Dai, and K. E. Trenberth, 2007: Hydroclimatic trends in the Mississippi River basin from 1948-2004. *J. Climate*, **20**, 4599-4614.

Robson, A. J., 2002: Evidence for trends in UK flooding. *Phil. Trans. Roy. Soc. London Series a-Math. Phys. Eng. Sciences*, **360,** 1327-1343.

Shiklomanov, A. I., T. I. Yakovleva, R. B. Lammers, I. P. Karasev, C. J. Vörösmarty, and E. Linder, 2006: Cold region river discharge uncertainty - estimates from large Russian rivers. *J. Hydrology*, **326,** 231-256.

Smith, L. C., 2000: Trends in Russian Arctic river-ice formation and breakup: 1917 to 1994. *Physical Geography*, **21,** 46-56.

Sun, Y., S. Solomon, A. Dai, and R. Portmann, 2007: How often will it rain? *J. Climate*, **20**, 4801-4818.

Trenberth, K. E. and J. W. Hurrell, 1994: Decadal atmosphere-ocean variations in the Pacific. *Climate Dynamics*, **9,** 303-319.

Trenberth, K. E., 1997: The definition of El Niño. *Bull. Amer. Meteorol. Soc.,* **78**, 2771-2777.

Trenberth, K.E., J.M. Caron, D.P. Stepaniak, and S. Worley, 2002: Evolution of El Niño-Southern Oscillation and global atmospheric surface temperatures, *J. Geophys. Res.*, *107*, 4065, doi:10.1029/2000JD000298.

Trenberth, K. E., and A. Dai, 2007: Effects of Mount Pinatubo volcanic eruption on the hydrological cycle as an analog of geoengineering. *Geophys. Res. Lett.*, **34,** L15702, doi:10.1029/2007GL030524.

Trenberth, K. E., L. Smith, T. Qian, A. Dai and J. Fasullo, 2007: Estimates of the global water budget and its annual cycle using observational and model data. *J. Hydrometeor.*, **8**, 758-769.

Vörösmarty, C. J., P. Green, J. Salisbury, and R. B. Lammers, 2000a: Global water resources: Vulnerability from climate change and population growth. *Science*, **289,** 284-288.

Vörösmarty, C. J., B. M. Fekete, M. Meybeck, and R. B. Lammers, 2000b: Global system of rivers: Its role in organizing continental land mass and defining land-to-ocean linkages. *Global Biogeochemical Cycles*, **14,** 599-621.

Woodward, W. A. and H. L. Gray, 1993: Global Warming and the Problem of Testing for Trend in Time-Series Data. *J. Climate*, **6,** 953-962.

Xiong, L. H., and S. L. Guo, 2004: Trend test and change-point detection for the annual discharge series of the Yangtze River at the Yichang hydrological station. *Hydrologic Sciences J.*, **49,** 99-112.

Yang, D., B. Ye, and D. L. Kane, 2004a: Streamflow changes over Siberian Yenisei River Basin. *J. Hydrology*, **296,** 59-80.

Yang, D. Q., B. S. Ye, and A. Shiklomanov, 2004b: Discharge characteristics and changes over the Ob River watershed in Siberia. *J. Hydrometeor.*, **5,** 595-610.

Ye, B. S., D. Q. Yang, and D. L. Kane, 2003: Changes in Lena River streamflow hydrology: Human impacts versus natural variations. *Water Resources Res.*, **39,** 1200, doi:10.1029/2003WR001991.

Zhang, X. B., K. D. Harvey, W. D. Hogg, and T. R. Yuzyk, 2001: Trends in Canadian streamflow. *Water Resources Res.*, **37,** 987-998.

Figure Captions:

FIG. 1. Distribution of the farthest downstream gauge stations (dots) for world's largest 925 rivers included in this study. Also shown are the world's major river systems as simulated by the CLM3. The color of the dots indicates the record length at the station during 1948-2004.

FIG. 2. Time series of observed yearly (Oct-Sep) streamflow (thick solid line), basin-averaged precipitation (dashed line, based on CRU_TS_2.10 data set (Mitchell and Jones 2005), and % of the basin area covered by rain-gauges (i.e. within 450 km of a gauge, thin solid curve, right ordinate) for (**a**) Amazon river (streamflow at station Obidos) and (**b**) Congo river (streamflow at station Kinshasa). The shading indicates the time period during which records from another station were used to infill the streamflow data gap through linear regression. The correlation coefficient between the streamflow and precipitation curves is also shown as r(P, V).

FIG. 3. Correlation coefficients, plotted against (**a**) long-term mean flow ($km^3\ yr^{-1}$) and (**b**) length of the gauge records, between observed and CLM3-simulated annual (water-year) streamflow at the farthest downstream stations for 576 rivers with 15 or more years of data and the correlation is statistically significant at the 5% level. Also shown in (b) are the 5% (solid line) and 1% (dashed line) significance levels (from Crow et al. 1960).

FIG. 4. Flowchart of the regression ($y = a + bx$) between observed (y) and CLM3-simulated (x) streamflow for the 925 rivers that is used to estimate the streamflow for months without data. Depending on the y record length (N, in months) and whether the correlation coefficient (R) between y and x is statistically significant (i.e., $|R| \geq Rs$, the lowest R that is significant at the 5% level), the regression was divided into c00-c09 categories. Note: the subscripts for R are defined as follows: *a* for annual time series, *m* for individual monthly time series, *am* for all-month-together time series, and *lag* for maximum lag correlation with a lag up to ±5 months. *M* is the number of months with valid regression. *All-mon. regr*. means that the regression was done with 12-month-

combine time series. The % numbers in parentheses indicate the cases occurred for the category. In category c01, spline interpolation was used to estimate the values for the missing months based on the data for the others.

F**IG. 5**. Time series of water-year (1 Oct. to 30 Sep.) streamflow (km^3 yr^{-1}) at the farthest downstream station (in parentheses) for world's 24 largest rivers from observations (thick solid line, left ordinate), the CLM3 simulation (dashed line, right ordinate), and the regression (thin solid line, left ordinate). The shading indicates the time period during which records from another station were used to infill the streamflow data gap through linear regression.

FIG. 6. Linear trends of yearly streamflow during 1948-2004 plotted as a function of the 1948-2004 mean flow rate of the corresponding river. The trend was divided by the long-term mean and is in % of the mean per decade, with the statistically significant trends (at 5% level) denoted by stars and insignificant ones by open circles (based on the test described in Woodward and Gray 1993).

FIG. 7. Time series of annual (water-year) freshwater discharge (in 0.1Sv; 1 Sv=10^6 m^3 s^{-1} = 31.56 $\times 10^3$ km^3 yr^{-1}) from land into the individual and global oceans from 1948-2004 estimated using the observed streamflow with data gaps infilled with CLM3-simulated flow (solid line) and infilled with the long-term mean (dashed line). Runoff from areas not monitored by the 925 rivers is not accounted for in these estimates (but included in Figs. 9-10). Also shown is the correlation coefficient (*r*) between the two curves.

FIG. 8. Linear trends from 1948-2004 in annual (water-year) (a) discharge from each 4^o lat × 5^o lon coastal box estimated from available gauge records and reconstructed river flow, (b) the runoff trend inferred from the discharge trend shown in (a), observed surface air temperature (c) and precipitation (d) (from Qian et al. 2006), CLM3-simulated snow cover (e) and soil ice water. The bottom row shows the confidence level (%) for (g) the discharge and (h) runoff trends based on a t-test. A 95% confidence means the trend is statistically significant at the 5% level.

FIG. 9. Time series of annual (water-year) freshwater discharge (solid line, in 0.1Sv; 1 Sv = 10^6 m^3 s^{-1} = 31.56 $\times 10^3$ km^3 yr^{-1}) from land into the individual and global oceans from 1948-2004. The shading indicates the ± one standard error, which includes the regression error and the observational error (estimated as the difference between the observed and the estimated river flow using the regression equation and CLM-simulated flow). Also shown (dashed, read on the right ordinate) is the Nino 3.4 SST index (Trenberth 1997; multiplied by -1) averaged over the 12 month period that yields a maximum correlation (r, negative) with the discharge data (see text for details). The linear slope (*b*) and its attained significance level (*p(b)*) of the discharge time series are given on top of each panel.

FIG. 10. Time series of annual (water-year) discharge (D, solid line) from 1948-2004 compared with observed water-year precipitation (P, dashed line, from Qian et al. 2006) averaged over the drainage areas of the individual and global oceans. The correlation coefficients among the two lines are given on top of each panel. The slope (*b*) and its attained probability (*p*) for the discharge are also shown. For Arctic drainage basin, another estimate of precipitation (long-dashed line, from CRU_TS_2.10 data set (Mitchell and Jones 2005)) is shown.

FIG. 11. Observed precipitation (top row) and CLM3-simulated runoff (bottom row) anomalies (in mm day^{-1}, relative to 1948-2004 mean) for the water year 1974 (left column) and 1992 (right column).

TABLE 1. The 1948-2004 mean annual streamflow ($km^3\ yr^{-1}$) at the downstream station from observations (V_{obs}) and CLM3 simulations (V_{clm}), its linear trend ($km^3\ yr^{-2}$) during 1948-2004 from observations (b_{obs}) and CLM3 simulations (b_{clm}), and the correlation coefficient (r) between the observed and CLM3-simulated annual flow for world's top 24 rivers shown in Figure 5. Gaps in observational records are filled with the simulated flow through regression in the mean and trend calculations but are unfilled in the correlation calculation. The significant trends and correlations at the 5% level are in **bold**. The numbering in the 1st column (#) is based on the river mouth outflow estimated by Dai and Trenberth (2002). The last column (T) indicates the time period during which the observational record was derived using observations at a nearby or upstream station through linear regression for some of the rivers.

# River (Station)	V_{obs}	V_{clm}	b_{obs}	b_{clm}	*r*	T
1. Amazon (Obidos)	5444	3228	-2.93	-4.10	**0.79**	8/1948-1/1968
2. Congo (Kinshasa)	1270	1089	**-3.59**	**-8.72**	**0.67**	1/1984-12/1999
3. Orinoco (Pte Angostu)	996	814	0.44	-0.07	**0.59**	
4. Changjiang (Datong)	907	838	-0.93	**-1.69**	**0.82**	
5. Brahmaputra (Bahaduradad)	643	399	0.98	-0.35	**0.52**	
6. Mississippi (Vicksburg)	552	651	**1.82**	1.31	**0.91**	
7. Yenisey (Igarka)	588	493	**1.58**	**-0.81**	0.31	
8. Paraná (Timbues)	517	692	**4.19**	0.67	**0.63**	9/1994-12/2006
9. Lena (Kusur)	532	396	0.24	**-1.04**	**0.54**	
10. Mekong (Pakse)	312	187	-0.28	**-0.96**	**0.78**	
11. Tocantins (Tucurui)	347	486	0.07	-0.74	**0.76**	2/1989-12/2006
12. Ob (Salekhard)	402	533	0.39	0.62	**0.77**	
13. Ganges (Farakka)	371	465	**-1.40**	**-1.63**	**0.70**	1/1976-12/2000
14. Irrawaddy (Sagaiing)	272	243	-0.32	-0.55	**0.57**	
15. St. Lawrence (Cornwall)	230	400	0.37	0.00	**0.55**	
16. Amur (Komsomolsk)	307	367	-0.89	**-1.87**	**0.84**	
17. Mackenzie (Artic Red)	286	259	-0.22	-0.51	**0.63**	
18. Xijiang (Wuzhou)	207	172	-0.63	-0.31	**0.88**	
19. Columbia (Dalles)	167	226	**-0.54**	0.35	**0.75**	
20. Magdalena (Calamar)	224	193	0.06	**-0.7**5	**0.68**	
21. Uruguay (Concordia)	182	67	**0.87**	**0.48**	**0.86**	4/1942-12/1964, 1/1980-12/2006
22. Yukon (Pilot Station)	200	275	0.13	-0.52	**0.60**	10/1956-9/1975, 10/1996-3/2001
23. Danube (Ceatal Izma)	204	208	0.12	-0.58	**0.85**	
24. Niger (Lokoja)	181	185	**-0.53**	**-1.74**	**0.60**	

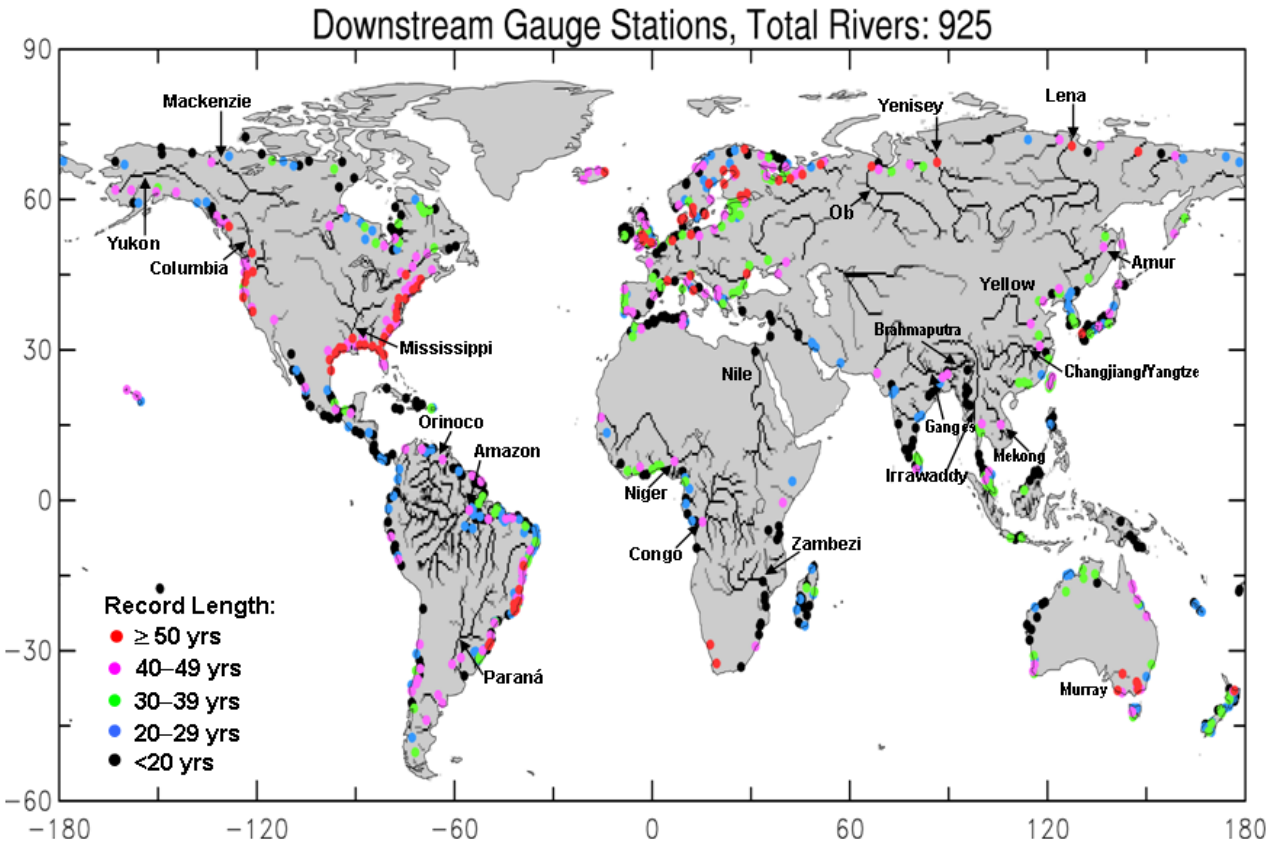

FIG. 1. Distribution of the farthest downstream gauge stations (dots) for world's largest 925 rivers included in this study. Also shown are the world's major river systems as simulated by the CLM3. The color of the dots indicates the record length at the station during 1948-2004.

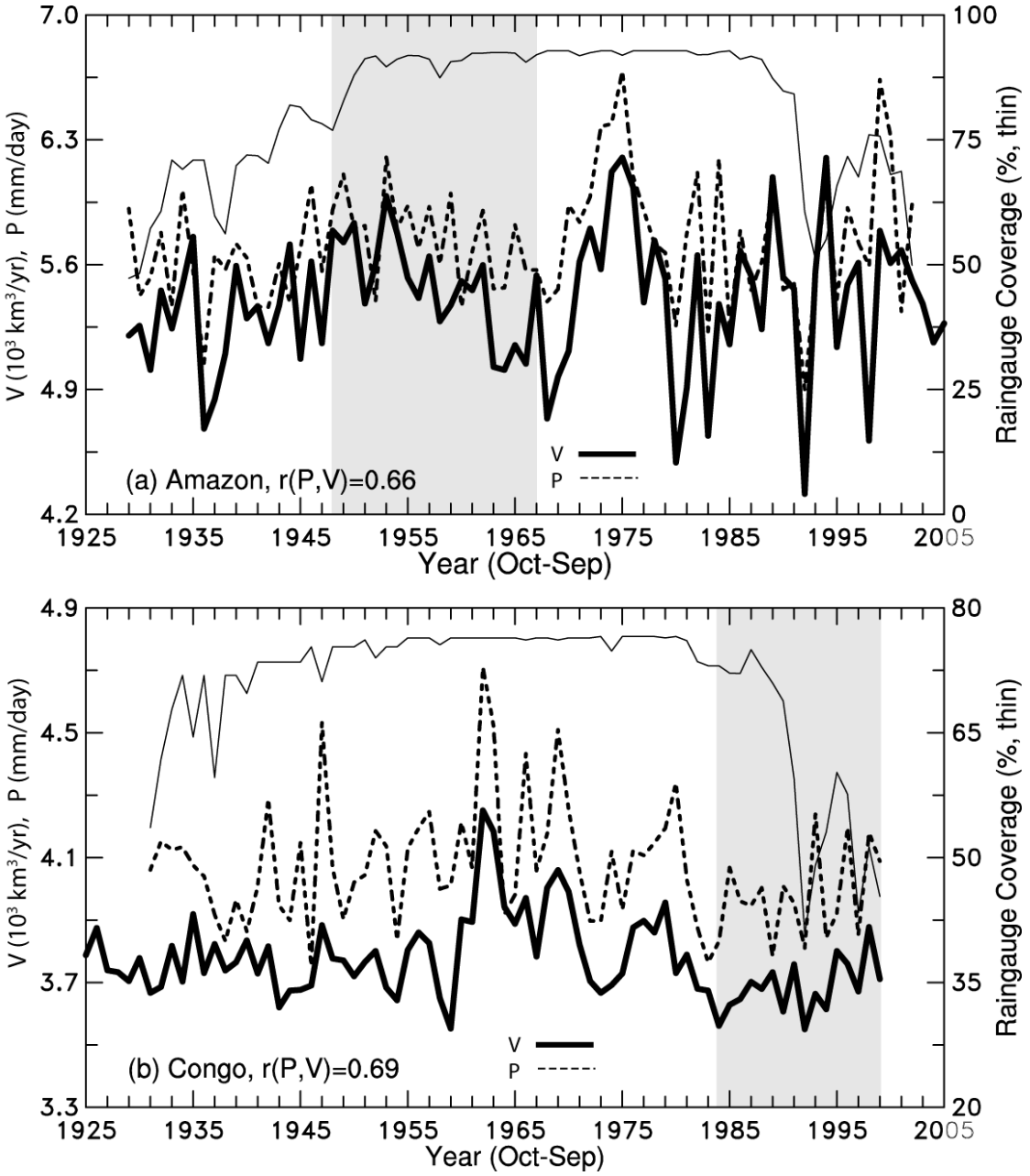

FIG. 2. Time series of observed yearly (Oct-Sep) streamflow (V, thick solid line), basin-averaged precipitation (P, dashed line, based on CRU_TS_2.10 data set (Mitchell and Jones 2005), and % of the basin area covered by rain-gauges (i.e. within 450 km of a gauge, thin solid curve, right ordinate) for (**a**) Amazon river (streamflow at station Obidos) and (**b**) Congo river (streamflow at station Kinshasa). The shading indicates the time period during which records from another station were used to infill the streamflow data gap through linear regression. The correlation coefficient between the streamflow and precipitation curves is also shown as r(P, V).

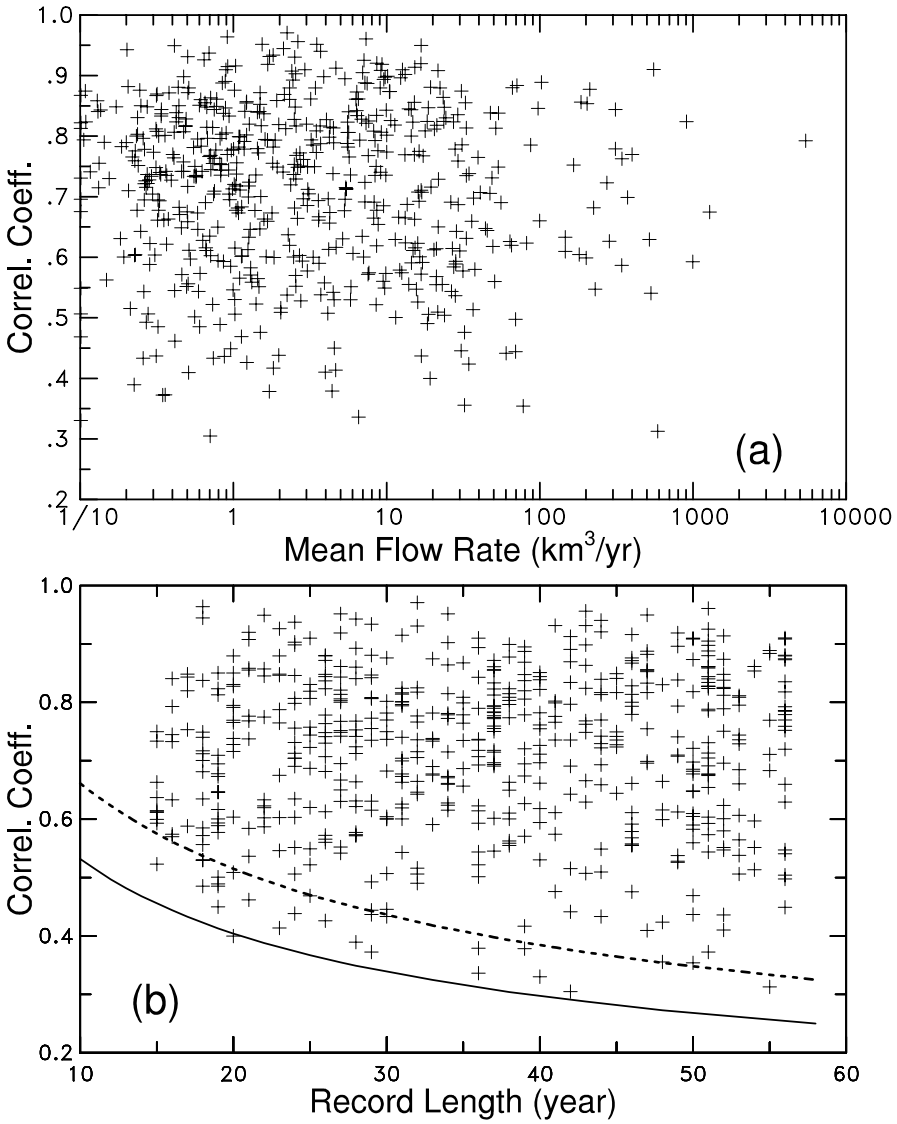

FIG. 3. Correlation coefficients, plotted against (**a**) long-term mean flow ($km^3\ yr^{-1}$) and (**b**) length of the gauge records, between observed and CLM3-simulated annual (water-year) streamflow at the farthest downstream stations for 576 rivers with 15 or more years of data and the correlation is statistically significant at the 5% level. Also shown in (b) are the 5% (solid line) and 1% (dashed line) significance levels (from Crow et al. 1960).

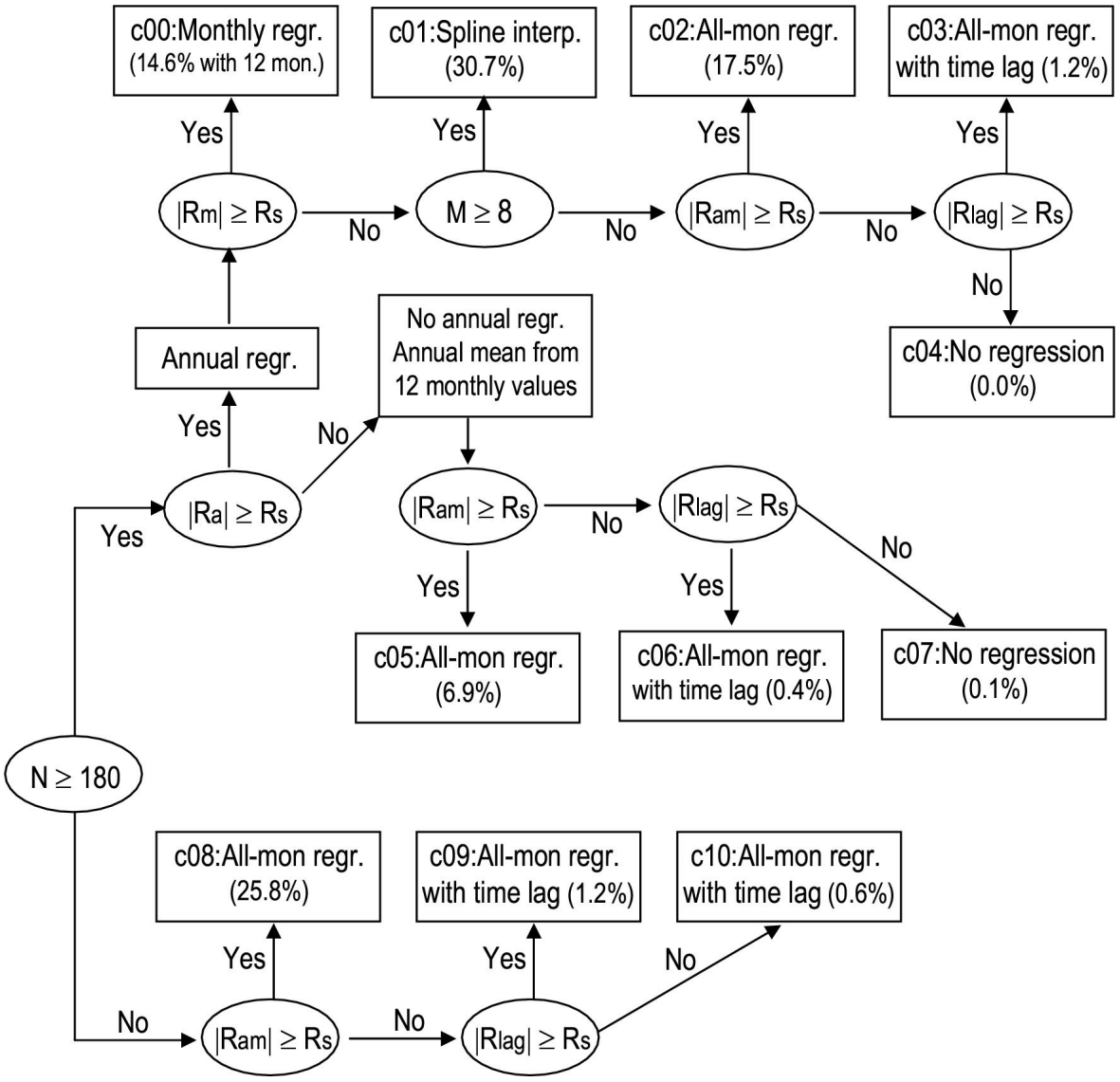

FIG. 4. Flowchart of the regression ($y = a + bx$) between observed (y) and CLM3-simulated (x) streamflow for the 925 rivers that is used to estimate the streamflow for months without data. Depending on the y record length (N, in months) and whether the correlation coefficient (R) between y and x is statistically significant (i.e., $|R| \geq Rs$, the lowest R that is significant at the 5% level), the regression was divided into c00-c09 categories. Note: the subscripts for R are defined as follows: *a* for annual time series, *m* for individual monthly time series, *am* for all-month-together time series, and *lag* for maximum lag correlation with a lag up to ±5 months. *M* is the number of months with valid regression. *All-mon. regr*. means that the regression was done with 12-month-combine time series. The % numbers in parentheses indicate the cases occurred for the category. In category c01, spline interpolation was used to estimate the values for the missing months based on the data for the others.

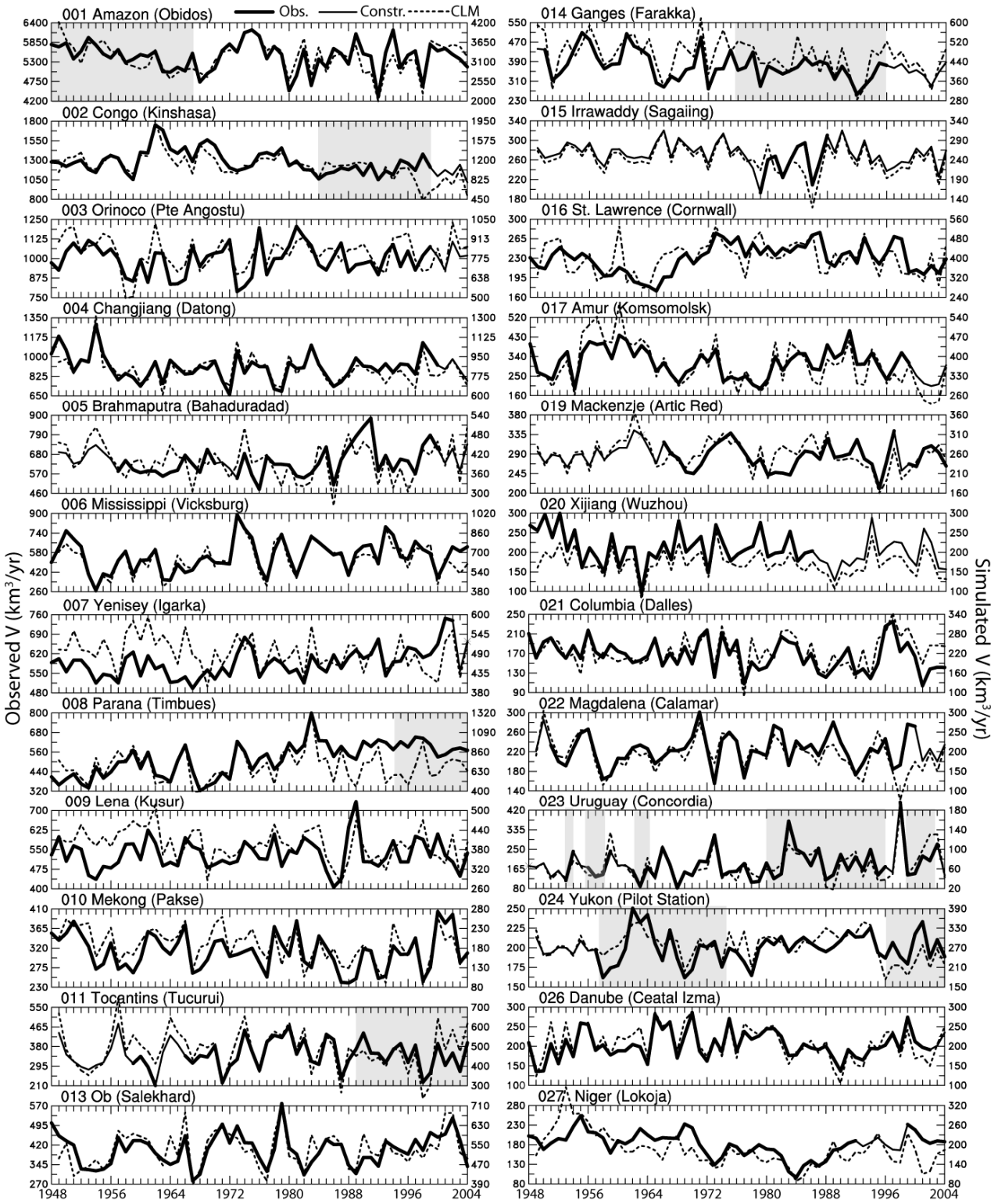

F**IG. 5**. Time series of water-year (1 Oct. to 30 Sep.) streamflow (km^3 yr^{-1}) at the farthest downstream station (in parentheses) for world's 24 largest rivers from observations (thick solid line, left ordinate), the CLM3 simulation (dashed line, right ordinate), and the regression (thin solid line, left ordinate). The shading indicates the time period during which records from another station were used to infill the streamflow data gap through linear regression.

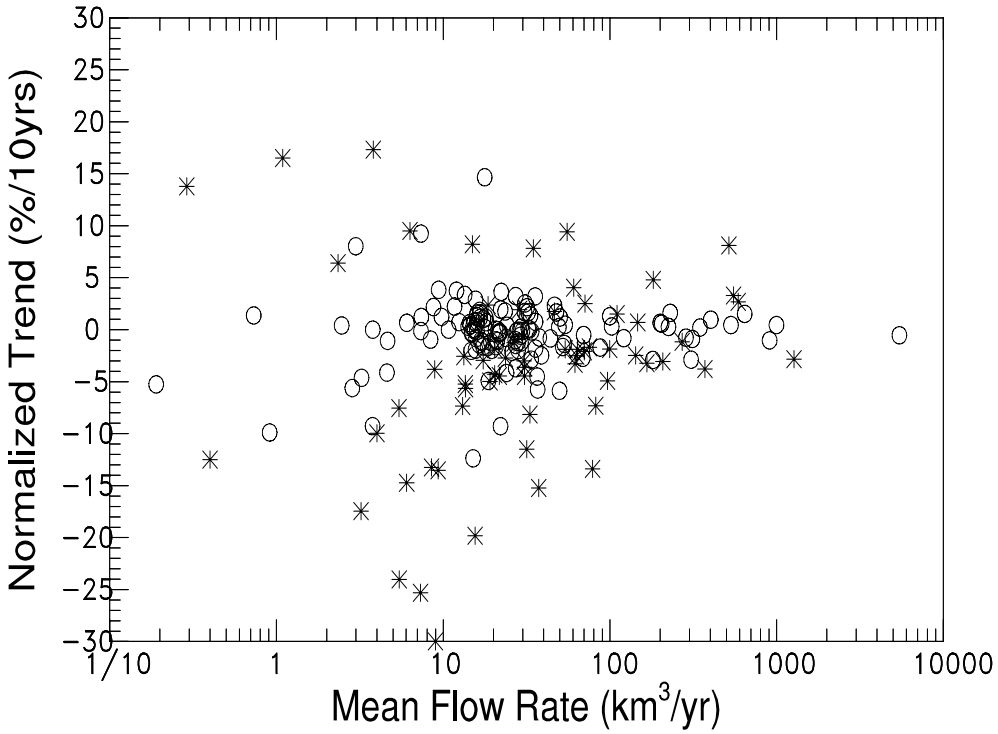

FIG. 6. Linear trends of yearly streamflow during 1948-2004 plotted as a function of the 1948-2004 mean flow rate of the corresponding river. The trend was divided by the long-term mean and is in % of the mean per decade, with the statistically significant trends (at 5% level) denoted by stars and insignificant ones by open circles (based on the test described in Woodward and Gray 1993).

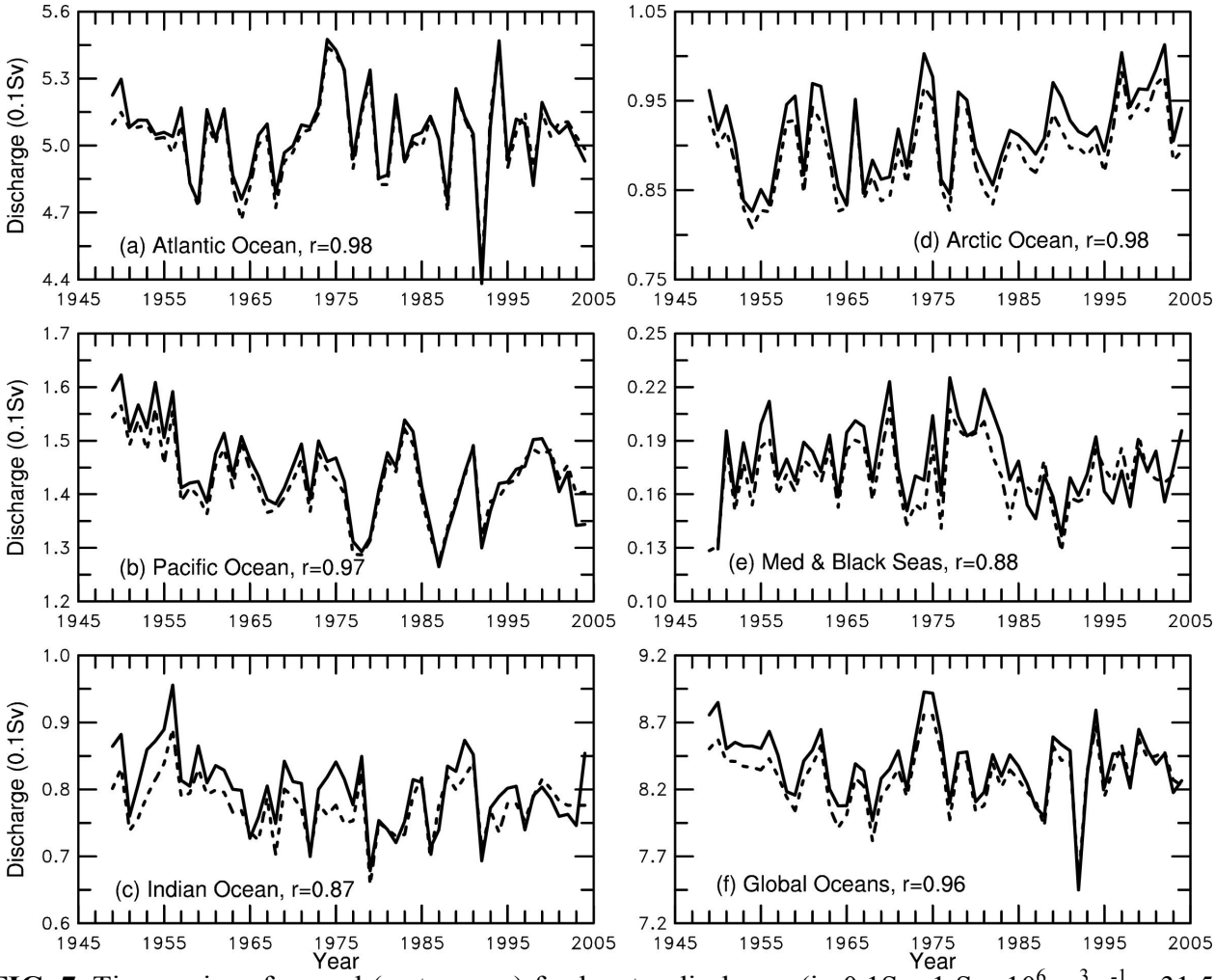

FIG. 7. Time series of annual (water-year) freshwater discharge (in 0.1Sv; 1 Sv=10^6 m^3 s^{-1} = 31.56 $\times 10^3$ km^3 yr^{-1}) from land into the individual and global oceans from 1948-2004 estimated using the observed streamflow with data gaps infilled with CLM3-simulated flow (solid line) and infilled with the long-term mean (dashed line). Runoff from areas not monitored by the 925 rivers is not accounted for in these estimates (but included in Figs. 9-10). Also shown is the correlation coefficient (*r*) between the two curves.

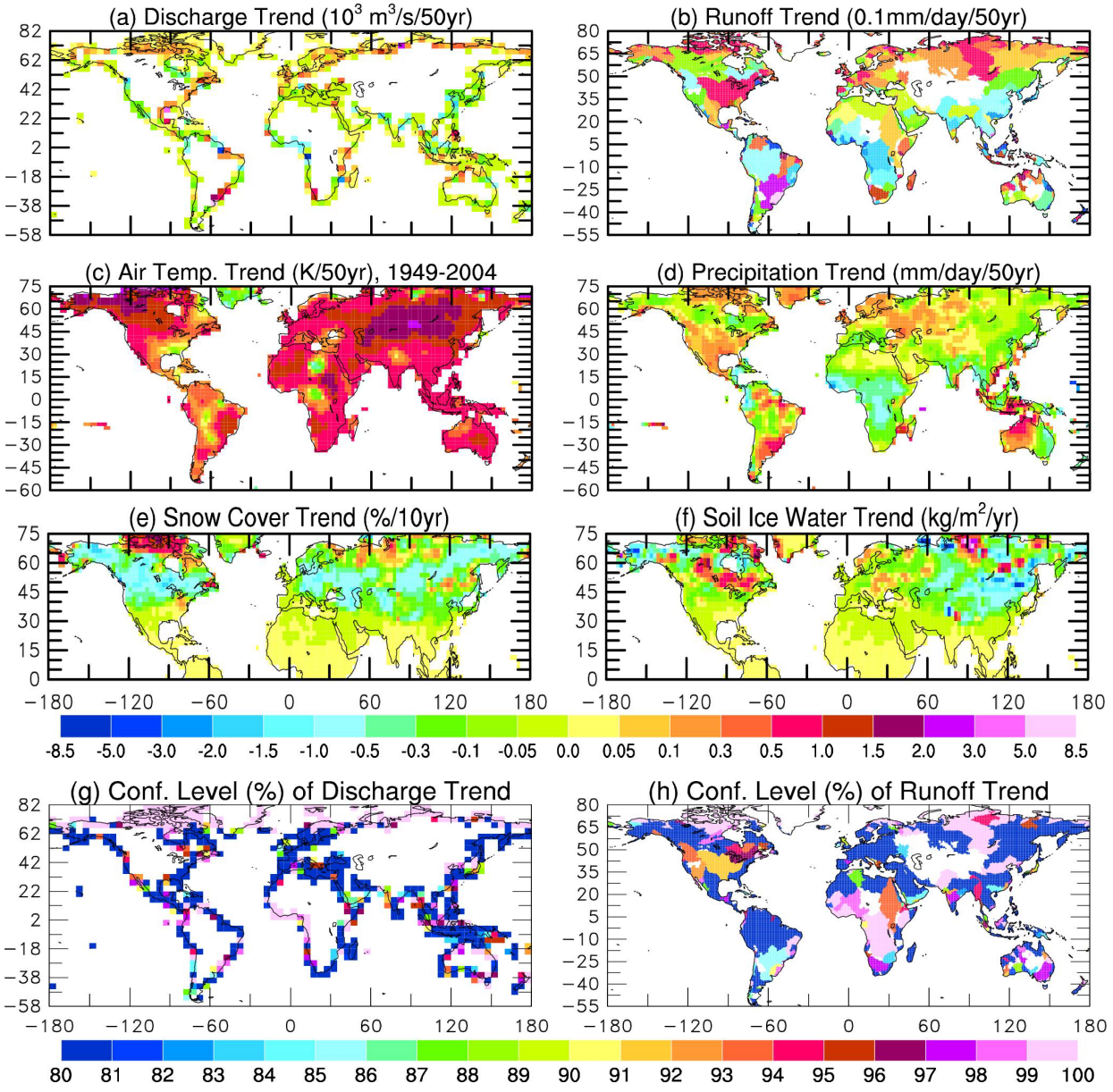

FIG. 8. Linear trends from 1948-2004 in annual (water-year) (a) discharge from each 4° lat × 5° lon coastal box estimated from available gauge records and reconstructed river flow, (b) the runoff trend inferred from the discharge trend shown in (a), observed surface air temperature (c) and precipitation (d) (from Qian et al. 2006), CLM3-simulated snow cover (e) and soil ice water. The bottom row shows the confidence level (%) for (g) the discharge and (h) runoff trends based on a t-test. A 95% confidence means the trend is statistically significant at the 5% level.

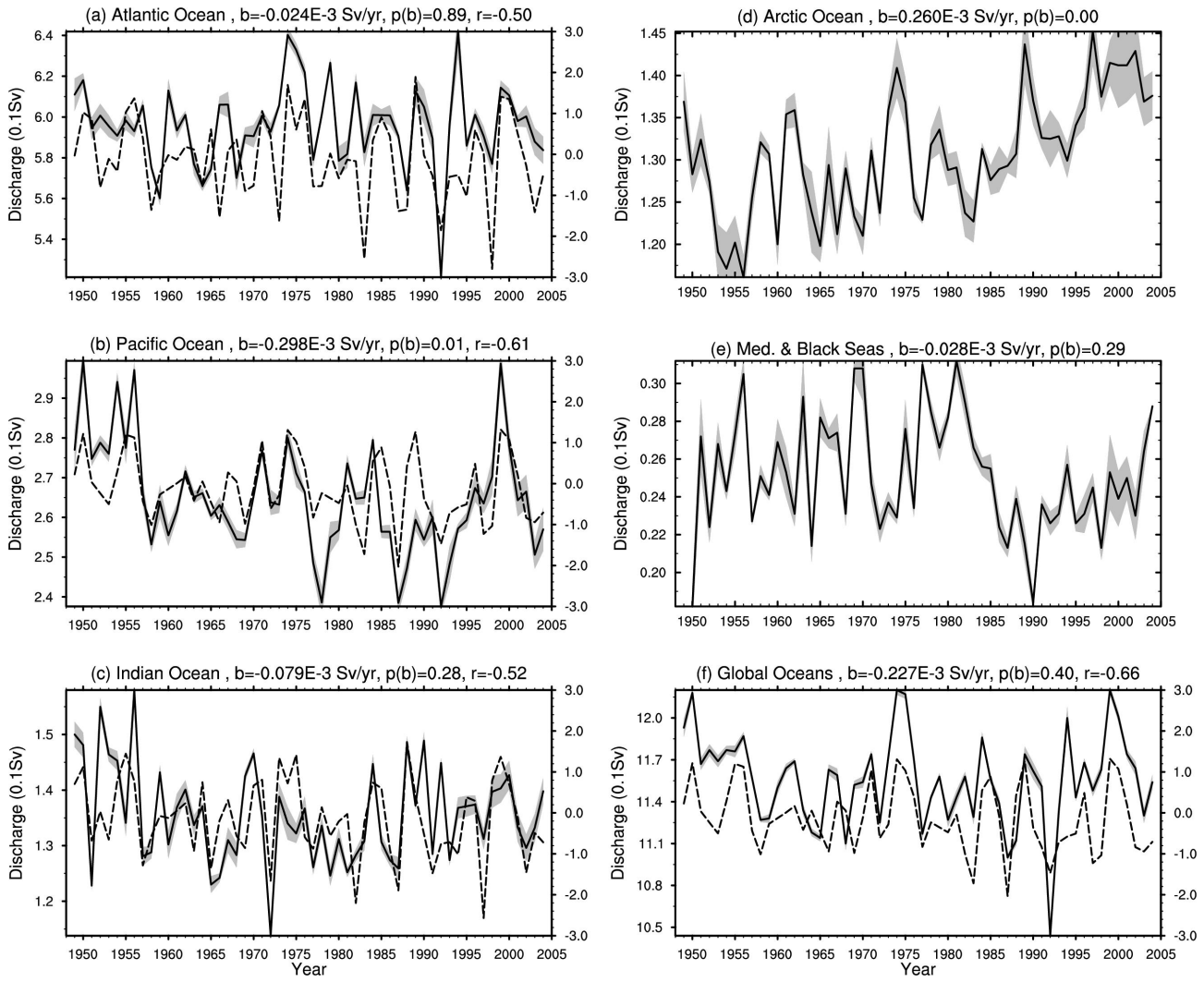

FIG. 9. Time series of annual (water-year) freshwater discharge (solid line, in 0.1Sv; 1 Sv = 10^6 m^3 s^{-1} = 31.56 $\times 10^3$ km^3 yr^{-1}) from land into the individual and global oceans from 1948-2004. The shading indicates the ± one standard error, which includes the regression error and the observational error (estimated as the difference between the observed and the estimated river flow using the regression equation and CLM-simulated flow). Also shown (dashed, read on the right ordinate) is the Nino 3.4 SST index (Trenberth 1997; multiplied by -1) averaged over the 12 month period that yields a maximum correlation (r, negative) with the discharge data (see text for details). The linear slope (*b*) and its attained significance level (*p(b)*) of the discharge time series are given on top of each panel.

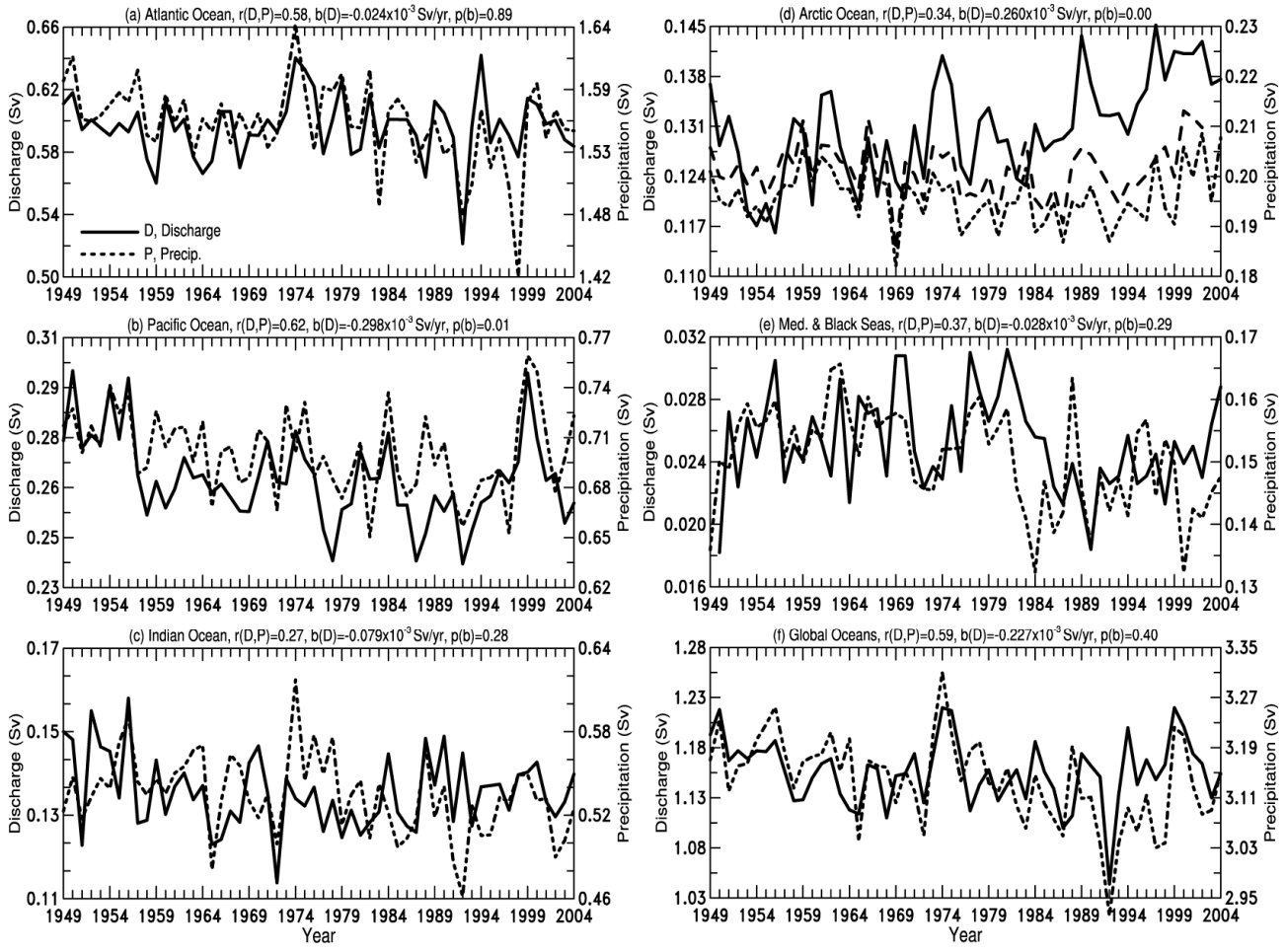

FIG. 10. Time series of annual (water-year) discharge (D, solid line) from 1948-2004 compared with observed water-year precipitation (P, dashed line, from Qian et al. 2006) averaged over the drainage areas of the individual and global oceans. The correlation coefficients among the two lines are given on top of each panel. The slope (*b*) and its attained probability (*p*) for the discharge are also shown. For Arctic drainage basin, another estimate of precipitation (long-dashed line, from CRU_TS_2.10 data set (Mitchell and Jones 2005)) is shown.

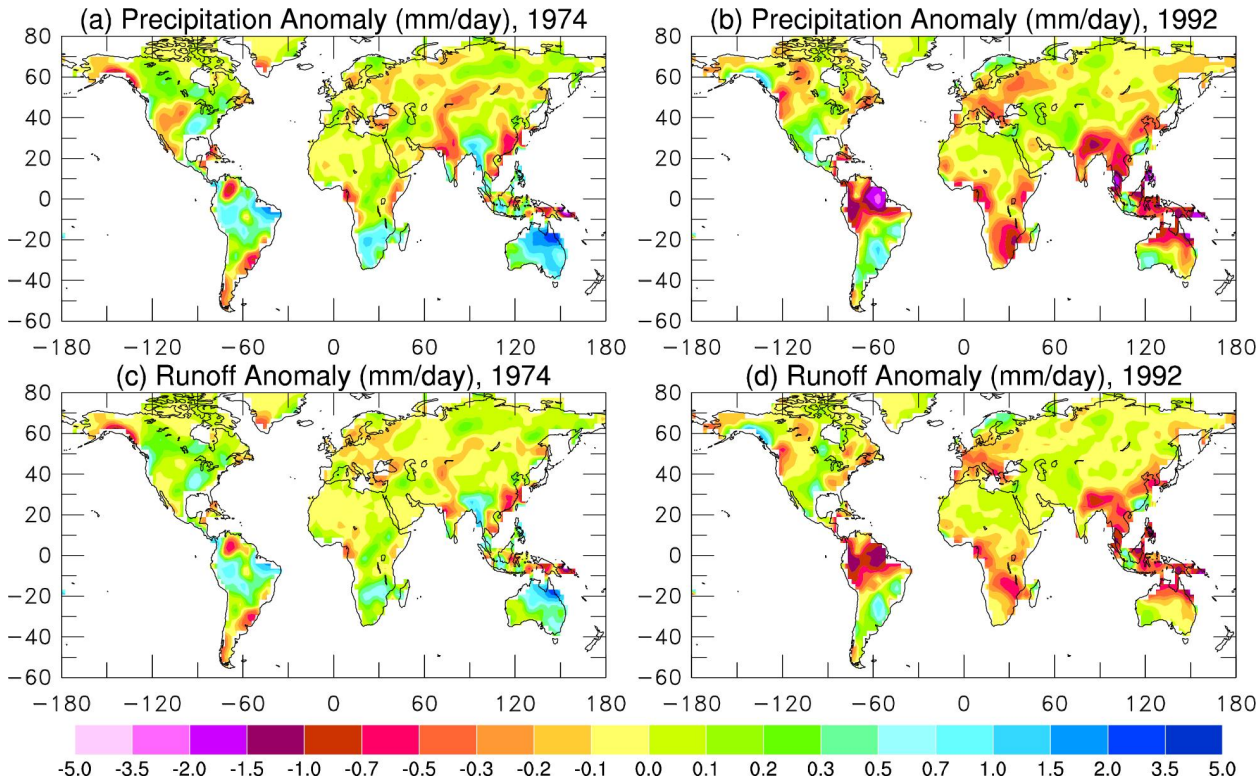

FIG. 11. Observed precipitation (top row) and CLM3-simulated runoff (bottom row) anomalies (in mm day^{-1}, relative to 1948-2004 mean) for the water year 1974 (left column) and 1992 (right column).